

# The Jacobian of a Riemann surface and the geometry of the cut locus of simple closed geodesics

Bjoern Muetzel \*

Department of Mathematics, Université Montpellier 2, place Eugène Bataillon,  
34095 Montpellier cedex 5, France

4th October 2019

## Abstract

To any compact Riemann surface of genus  $g$  one may assign a principally polarized abelian variety of dimension  $g$ , the *Jacobian* of the Riemann surface. The Jacobian is a complex torus, and a Gram matrix of the lattice of a Jacobian is called a *period Gram matrix*. This paper provides upper and lower bounds for all the entries of the period Gram matrix with respect to a suitable homology basis. These bounds depend on the geometry of the cut locus of non-separating simple closed geodesics. Assuming that the cut loci can be calculated, a theoretical approach is presented followed by an example where the upper bound is sharp. Finally we give practical estimates based on the Fenchel-Nielsen coordinates of surfaces of signature  $(1, 1)$ , or *Q-pieces*. The methods developed here have been applied to surfaces that contain small non-separating simple closed geodesics in [BMMS].

Keywords : Riemann surfaces, Jacobians, harmonic forms, energy, hyperbolic geometry.

Mathematics Subject Classifications (2010): 14H40, 14H42, 30F15 and 30F45.

## 1 Introduction

Let  $S$  be a hyperbolic Riemann surface of genus  $g \geq 2$ . We call a set of  $2g$  oriented simple closed geodesics

$$A = (\alpha_1, \alpha_2, \dots, \alpha_{2g-1}, \alpha_{2g})$$

a *canonical basis*, if

- for each  $\alpha_i$  there exists exactly one  $\alpha_{\tau(i)} = \begin{cases} \alpha_{i+1} & \text{if } i \text{ odd} \\ \alpha_{i-1} & \text{if } i \text{ even} \end{cases} \in A$  that intersects  $\alpha_i$  in exactly one point.

- the curves are oriented in a way, such that

$$\text{Int}(\alpha_i, \alpha_{i+1}) = 1 \text{ for all } i = 1, 3, \dots, 2g - 1,$$

where  $\text{Int}(\cdot, \cdot)$  denotes the algebraic intersection number.

---

\*E-mail address : bjorn.muetzel@gmail.com

Note that  $A$  can be called a basis as the homology classes  $([\alpha_i])_{i=1,\dots,2g} \subset H_1(S, \mathbb{Z})$  form a basis of  $H_1(S, \mathbb{R})$  as a vector space.

In the vector space of real harmonic 1-forms on  $S$ , let  $(\sigma_k)_{k=1,\dots,2g}$  be the *dual basis* for  $([\alpha_i])_{i=1,\dots,2g} \subset H_1(S, \mathbb{Z})$  defined by

$$\int_{[\alpha_i]} \sigma_k = \delta_{ik}.$$

A *period Gram matrix*  $P_S$  (with respect to  $A$ ) of  $S$  is the Gram matrix

$$P_S = (\langle \sigma_i, \sigma_j \rangle)_{i,j=1,\dots,2g} = \left( \int_S \sigma_i \wedge {}^* \sigma_j \right)_{i,j=1,\dots,2g}.$$

This period matrix  $P_S$  defines a complex torus, the *Jacobian* or *Jacobian variety*  $J(S)$  of the Riemann surface  $S$  (see [FK], chapter III). Let

$$E(\sigma_i) = E_S(\sigma_i) = \int_S \sigma_i \wedge {}^* \sigma_i = \langle \sigma_i, \sigma_i \rangle$$

be the *energy* of  $\sigma_i$  (over  $S$ ). As  $P_S$  is a Gram matrix,  $E(\sigma_i)$  is also the squared norm of a vector  $v_i$  in the lattice of the Jacobian. By Riemann's period relations the Jacobian is a principally polarized abelian variety (see [BL], Section 4.1 for a definition). The lattices of principally polarized abelian varieties are exactly the symplectic lattices ([BS]). The Schottky problem is to characterize the Jacobians among the principally polarized abelian varieties.

Buser and Sarnak ([BS]) approached this problem by means of a geometric invariant:

The squared norm of the shortest non-zero vector in the lattice of a Jacobian of a Riemann surface of genus  $g \geq 2$  is bounded from above by  $\log(4g)$ , whereas it can be of order  $g$  for the lattice of a principally polarized abelian variety of dimension  $g$ . Recently, more insight has been obtained into the connection between the global geometry of a compact Riemann surface of genus  $g$  and the geometry of its Jacobian. In [BPS] the  $\log(g)$ -bound on the squared norm of a lattice vector of the Jacobian has been further extended to almost  $g$  linearly independent vectors. In [Mu2] it was shown that, for the case of a hyperelliptic surface, the squared norm of the shortest lattice vector is bounded from above by a constant independent of the genus.

In this paper, we examine the connection between the metric, hyperbolic geometry of a compact Riemann surface, and the geometry of its Jacobian. In previous papers (see [BSi] or [Se]), this approach has been taken for special cases, for example when the Riemann surface is a real algebraic curve. For these special cases, there exist algorithms to calculate the period matrix. The aim of this paper is to find upper and lower bounds for all entries of the period Gram matrix given with respect to a canonical basis, based on the hyperbolic metric of an arbitrary compact Riemann surface. The bounds depend on the geometry of the cut loci of these curves and related simple closed geodesics, and are obtained by estimating the energy of the corresponding dual harmonic forms.

After introducing the necessary tools and definitions in Section 2, we will present a theoretical approach in Section 3. Here we find upper bounds for the energy of the dual harmonic forms by estimating the capacity of hyperbolic tubes as follows.

Let  $T(\alpha_{\tau(i)}) \subset S$  be a topological tube, embedded in  $S$  obtained by a continuous deformation of

a small embedded cylinder  $C$  around  $\alpha_{\tau(i)}$ . The capacity of such a tube gives an upper bound for the energy  $E(\sigma_i)$  of  $\sigma_i$ . This is the diagonal entry  $p_{ii}$  of the period Gram matrix  $P_S$ :

$$\text{cap}(T(\alpha_{\tau(i)})) \geq E(\sigma_i) = p_{ii}.$$

In our theoretical approach, the boundary of such a tube will be provided by the cut locus of a simple closed geodesic of the canonical basis. This allows us to extend our tubes over the whole surface  $S$  and to obtain a lower bound on  $E(\sigma_i)$ . This bound is obtained using projections of vector fields onto curves. Let  $S_{\tau(i)}$  be the surface obtained by cutting open  $S$  along the cut locus  $CL(\alpha_{\tau(i)})$  of  $\alpha_{\tau(i)}$  (see (4)). Then

$$\text{cap}(S_{\tau(i)}) \geq p_{ii}.$$

Upper and lower bounds for the non-diagonal elements are obtained in a similar way.

The method presented in Section 3 relies on the premise that the cut loci in question can be calculated. This is illustrated by the following two examples. **Example 3.1** shows the limitations of the method, while **Example 3.2** shows a case where the upper bound is sharp.

**Example 1.1.** *Let  $N$  be a necklace surface of genus  $g \geq 2$  and  $A = (\alpha_i)_{i=1, \dots, 2g}$  a canonical basis. Let  $N_1$  be the surface obtained by cutting open  $N$  along the cut locus  $CL(\alpha_1)$  of  $\alpha_1$ . Let  $P_N = (p_{ij})_{i,j}$  be the period Gram matrix with respect to  $A$ . Then*

$$\frac{c_{\alpha_1}}{g-1} \geq p_{22} \geq 0 \quad \text{and} \quad \text{cap}(N_1) \geq p_{22}, \quad \text{but} \quad \text{cap}(N_1) \geq \frac{\ell(\alpha_1)}{\pi},$$

where  $c_{\alpha_1}$  is a factor that depends only on the fixed length  $\ell(\alpha_1)$  of  $\alpha_1$ .

Hence  $p_{22}$  is at most of order  $\frac{1}{g}$  and goes to zero, as  $g$  goes to infinity. Our upper bound, on the contrary, is always bigger than the constant  $\frac{\ell(\alpha_1)}{\pi}$ . This example shows an instance of the case where our upper bound cannot be of the right order.

**Example 1.2.** *Let  $L$  be a linear surface of genus  $g \geq 2$  and  $A = (\alpha_i)_{i=1, \dots, 2g}$  a canonical basis. Let  $L_1$  be the surface obtained by cutting open  $L$  along the cut locus  $CL(\alpha_1)$  of  $\alpha_1$ . Let  $P_L = (p_{ij})_{i,j}$  be the period Gram matrix with respect to  $A$ . Then for  $\epsilon_L > 0$*

$$p_{22} = \text{cap}(L_1) - \epsilon_L.$$

Note that  $\epsilon_L$  depends on the geometry of  $L$  and may become arbitrarily small.

This example shows an instance of the case where the bound is sharp for any genus.

The methods developed in this paper have been applied to surfaces that contain small simple closed geodesics in [BMMS]. We state this refined estimate here to enlarge the list of examples:

**Example 1.3.** [BMMS] *Let  $S$  be a Riemann surface of genus  $g \geq 2$ , that contains a separating simple closed geodesic  $\gamma$  of length  $\ell(\gamma) \leq \frac{1}{2}$ . Then  $\gamma$  separates the surface into two surfaces  $S^1$  and  $S^2$  of signature  $(g_1, 1)$  and  $(g_2, 1)$ . Let  $A = (\alpha_i)_{i=1, \dots, 2g}$  be a canonical basis of  $S$ , such that  $(\alpha_1, \dots, \alpha_{2g_1}) \subset S^1$  and  $(\alpha_{2g_1+1}, \dots, \alpha_{2(g_1+g_2)}) \subset S^2$ . Let  $P_S = (p_{ij})_{i,j}$  be the period Gram matrix with respect to  $A$ . Then*

$$|p_{ij}| = |p_{ji}| \leq \frac{2 \cdot (c_{\alpha_{\tau(i)}} + c_{\alpha_{\tau(j)}})}{|\log(\ell(\gamma))|} \quad \text{for} \quad j \in \{1, \dots, 2g_1\}, i \in \{2g_1 + 1, \dots, 2g\},$$

where  $c_{\alpha_{\tau(i)}}$  and  $c_{\alpha_{\tau(j)}}$  depend only on the length of  $\alpha_{\tau(i)}$  and  $\alpha_{\tau(j)}$ , respectively.

This means that the matrix  $P_S$  converges to a block matrix if  $\ell(\gamma)$  goes to zero. In this case the bound on a non-diagonal entry of  $P_S$  is sharp.

Finally, in Section 4 we present practical estimates based on the geometry of surfaces of signature  $(1, 1)$ , or  $Q$ -pieces embedded in  $S$ . Under this condition the cut loci of the elements of a canonical basis can be (at least partially) calculated. Estimates on the entries of a period Gram matrix will be computed based on the  $3g$  Fenchel-Nielsen coordinates (see Section 2.3) of these  $g$   $Q$ -pieces. Let

$$(\mathcal{Q}_i)_{i=1,3,\dots,2g-1} \subset S$$

be a set of  $Q$ -pieces, whose interiors are pairwise disjoint. Let  $\beta_i$  be the boundary geodesic of  $\mathcal{Q}_i$ ,  $\alpha_i$  an interior simple closed geodesic, and  $tw_i$  the twist parameter at  $\alpha_i$ . The geometry of  $\mathcal{Q}_i$  is determined by the Fenchel-Nielsen coordinates  $(\ell(\beta_i), \ell(\alpha_i), tw_i)$ . For technical reasons we assume furthermore that

$$\cosh\left(\frac{\ell(\alpha_i)}{2}\right) \leq \cosh\left(\frac{\ell(\beta_i)}{6}\right) + \frac{1}{2} \quad \text{for all } i \in \{1, 3, \dots, 2g-1\}. \quad (1)$$

Such a pair  $(\alpha_i, \beta_i)$  always exists, see [Pa], **Proposition 5.4**.

In Section 4, we first determine suitable  $\alpha_{\tau(i)} \subset \mathcal{Q}_i$  for each  $\alpha_i$ , such that the pairs  $((\alpha_i, \alpha_{\tau(i)}))_{i=1,3,\dots,2g-1}$  form a canonical basis. Now fix an  $i \in \{1, 3, \dots, 2g-1\}$ . Let  $\alpha_{i\tau(i)} \subset \mathcal{Q}_i$  be the simple closed geodesic in the free homotopy class of  $\alpha_i(\alpha_{\tau(i)})^{-1}$ . For  $j \in \{i, \tau(i), i\tau(i)\}$ , let

- $\beta_j = \beta_i$  be the boundary geodesic of  $\mathcal{Q}_i$ ,
- $tw_j$  the twist parameter at  $\alpha_j$ ,
- $FN_j := (\ell(\beta_j), \ell(\alpha_j), tw_j)$  the corresponding Fenchel-Nielsen coordinates of  $\mathcal{Q}_i$ .

In Section 4.1,  $FN_{\tau(i)}$  and  $FN_{i\tau(i)}$  are calculated from  $FN_i$ . Section 4.2 and 4.3 give explicit functions

$$\begin{aligned} f^u, f^l &: \mathbb{R}^+ \times \mathbb{R}^+ \times \left(-\frac{1}{2}, \frac{1}{2}\right] \rightarrow \mathbb{R}^+ \\ f^u &: FN_j \mapsto f^u(FN_j) \quad \text{and} \quad f^l: FN_j \mapsto f^l(FN_j), \end{aligned}$$

providing upper and lower bounds on all entries of  $P_S = (p_{ij})_{i,j}$  in the following way. For a diagonal entry  $p_{ii}$  we have:

$$f^l(FN_{\tau(i)}) \leq p_{ii} \leq \text{cap}(S_{\tau(i)} \cap \mathcal{Q}_i) \leq f^u(FN_{\tau(i)}).$$

Upper and lower bounds for the non-diagonal entries are provided in terms of simple linear combinations of the functions. These estimates are summarized in **Theorem 4.1**. An example of a period Gram matrix obtained via this method is given in **Example 4.3**:

**Example 1.4.** Let  $\mathcal{Q}_1$  and  $\mathcal{Q}_3$  be two isometric  $Q$ -pieces given in Fenchel-Nielsen coordinates  $FN_1$  and  $FN_3$ , respectively, where  $FN_i = (\ell(\beta_i), \ell(\alpha_i), tw_i) = (2, 1, 0.1)$  for  $i \in \{1, 3\}$ . Let  $S = \mathcal{Q}_1 + \mathcal{Q}_3$  be a Riemann surface of genus 2, which we obtain by gluing  $\mathcal{Q}_1$  and  $\mathcal{Q}_3$  along  $\beta_1$  and  $\beta_3$  with arbitrary twist parameter  $tw_\beta \in (-\frac{1}{2}, \frac{1}{2}]$ . Then there exists a canonical basis  $A = (\alpha_1, \dots, \alpha_4)$  and a corresponding period Gram matrix  $P_S$ , such that

$$\begin{pmatrix} 2.11 & -0.46 & -0.42 & -0.26 \\ -0.46 & 0.33 & -0.26 & -0.11 \\ -0.42 & -0.26 & 2.11 & -0.46 \\ -0.26 & -0.11 & -0.46 & 0.33 \end{pmatrix} \leq P_S \leq \begin{pmatrix} 2.53 & 0.20 & 0.42 & 0.26 \\ 0.20 & 0.44 & 0.26 & 0.11 \\ 0.42 & 0.26 & 2.53 & 0.20 \\ 0.26 & 0.11 & 0.20 & 0.44 \end{pmatrix}.$$

In Section 4.4, the results are summarized in *Table 1* and *2* and compared with the upper bound  $f_{simp}^u(FN_j)$  that can be obtained from the method in [BS] applied to Q-pieces. This bound is in general much larger than  $f^u(FN_j)$ .

We note that the upper bound  $f^u(FN_j)$  is close to the lower bound  $f^l(FN_j)$ , if a large part of the cut locus  $CL(\alpha_j)$  of  $\alpha_j$  is contained in  $\mathcal{Q}_i$  and if  $\ell(\alpha_j) \cdot |tw_j|$  is small. The first condition is fulfilled if the length  $\ell(\beta_i)$  of the boundary geodesic  $\beta_i$  is small, the second if both  $\ell(\alpha_j)$  and  $|tw_j|$  are small. This justifies the choice of  $\alpha_i$  in inequality (1). It is noteworthy that for  $|tw_j| = 0$  and  $\ell(\beta_i)$  small the estimates are almost sharp, independent of the length  $\ell(\alpha_j)$ .

Since the estimates for the entries of  $P_S$  are linear combinations of the functions  $(f^u(FN_j))_j$  and  $(f^l(FN_j))_j$ , the estimates are good if all Fenchel-Nielsen coordinates involved are small. Note that by [BSe2] there exists a canonical basis for a Riemann surface of genus  $g$ , where the largest element is of order  $g$ . Hence, at least the condition on the length of the geodesics involved can in principle be satisfied for small  $g$ .

The advantage of the method is that information about the geometry of the surface can be incorporated. Suppose, for example, that the geometry of  $\mathcal{Y}_1$ , the surface of signature  $(0, 3)$ , or *Y-piece*, attached to the Q-piece  $\mathcal{Q}_1$  is known. Then for  $j \in \{1, 2, 12\}$  the cut locus  $CL(\alpha_j) \cap (\mathcal{Q}_1 \cup \mathcal{Y}_1)$  can be calculated. Incorporating this information we obtain better estimates for the corresponding entries of the period Gram matrix. Information about isometries of the surface can also be incorporated. This is shown in **Example 3.2**.

## 2 Preliminaries

Many calculations presented in the following sections rely on the embedding of topological tubes around simple closed geodesics of Riemann surfaces into hyperbolic cylinders and subsequent approximations and calculations in Fermi coordinates. These concepts are presented in Section 2.1. To describe these tubes we make use of the geometry of hyperbolic polygons. The corresponding trigonometric formulas are given in Section 2.2. Finally, Section 2.3 presents the definition of the Fenchel-Nielsen coordinates used throughout the paper.

### 2.1 Fermi coordinates and capacity estimates

The Poincaré model of the hyperbolic plane is the following subset of the complex plane  $\mathbb{C}$ ,

$$\mathbb{H} = \{z = x + iy \in \mathbb{C} \mid y > 0\}$$

with the hyperbolic metric  $ds^2 = \frac{1}{y^2}(dx^2 + dy^2)$ .

*Fermi coordinates*  $\psi$ , with baseline  $\eta$  and base point  $p$ , are defined as follows: the Fermi coordinates are a bijective parametrization of  $\mathbb{H}$

$$\psi : \mathbb{R}^2 \rightarrow \mathbb{H}, \psi : (t, s) \mapsto \psi(t, s),$$

where  $\psi(0, 0) = p$ . Each point  $q = \psi(t, s) \in \mathbb{H}$  can be reached by starting from the base point  $p$  and moving along  $\eta$ , the directed distance  $t$  to  $\psi(t, 0)$ . There is a unique geodesic,  $\nu$ , intersecting  $\eta$  perpendicularly in  $\psi(t, 0)$ . From  $\psi(t, 0)$  we now move along  $\nu$  the directed distance  $s$  to  $\psi(t, s)$ .

A *hyperbolic cylinder*  $C$  or shortly *cylinder* is a set isometric to

$$\{\psi(t, s) \mid (t, s) \in [0, b] \times [a_1, a_2]\} \quad \text{mod} \quad \{\psi(0, s) = \psi(b, s) \mid s \in [a_1, a_2]\},$$

with the induced metric from  $\mathbb{H}$ . The baseline of  $C$  is the simple closed geodesic  $\gamma$  in  $C$ , which has length  $\ell(\gamma) = b$ .

Consider a cylinder  $C$ . Let  $U \subset C$  be a set and  $F \in \text{Lip}(\bar{U})$  a Lipschitz function on the closure of  $U$ . Let  $G$  be the metric tensor with respect to the Fermi coordinates. Then, the *energy of  $F$  on  $U$* ,  $E_U(F)$  is given by

$$E_U(F) = \iint_{\psi^{-1}(U)} \|D(F \circ \psi)\|_{G^{-1}}^2 \sqrt{\det(G)}.$$

Using Fermi coordinates, we obtain  $E_U(F)$  with  $F \circ \psi = f$ :

$$E_U(F) = \iint_{\psi^{-1}(U)} \frac{1}{\cosh(s)} \frac{\partial f(t, s)^2}{\partial t} + \cosh(s) \frac{\partial f(t, s)^2}{\partial s} ds dt \geq \iint_{\psi^{-1}(U)} \cosh(s) \frac{\partial f(t, s)^2}{\partial s}. \quad (2)$$

The *capacity* of an annulus  $R \subset C$ ,  $\text{cap}(R)$  is given by

$$\text{cap}(R) = \inf\{E_R(F) \mid \{F \in \text{Lip}(\bar{R}) \mid F|_{\partial_1 R} = 0, F|_{\partial_2 R} = 1\}\}.$$

In [Mu1], we obtain general upper and lower bounds on the capacity of annuli on a cylinder of constant curvature. These annuli are obtained by a continuous deformation of the cylinder itself. The upper bound is obtained by constructing a test function as explained next. We adapt the known harmonic function that solves the capacity problem for cylinders of a constant width to the boundary, using the parametrization of a cylinder in Fermi coordinates. We obtain a lower bound by determining explicitly the function  $p$ , that satisfies the boundary conditions of the capacity problem on  $R$  and minimizes the last integral in the above inequality (2). If the annulus  $R \subset C$  is given in Fermi coordinates by

$$R = \psi\{(t, s) \mid s \in [a_1(t), a_2(t)], t \in [0, \ell(\gamma)]\},$$

where  $a_1(\cdot)$  and  $a_2(\cdot)$  are piecewise differentiable functions with respect to  $t$ . Then by [Mu1], **Theorem 4.1** we have:

**Theorem 2.1.** *There exists a Lipschitz function  $\tilde{F} \in \text{Lip}(R)$ , such that for  $H(s) = 2 \arctan(\exp(s))$  and  $q_i(t) = \frac{\partial H(s_0)}{\partial s}|_{s_0=a_i(t)} \cdot a'_i(t)$  for  $i \in \{1, 2\}$ , we have:*

$$\int_{t=0}^{\ell(\gamma)} \frac{1 + \frac{q_1(t)^2 + q_1(t)q_2(t) + q_2(t)^2}{3}}{H(a_2(t)) - H(a_1(t))} dt = E(\tilde{F}) \geq \text{cap}(R) \geq \int_{t=0}^{\ell(\gamma)} \frac{1}{H(a_2(t)) - H(a_1(t))} dt.$$

The estimate is sharp if the boundary is constant. In this case,  $a_1(t) = a_1$ ,  $a_2(t) = a_2$ , and  $R = C'$  is itself an embedded cylinder. Especially, for  $a_1 = -a_2$ , this simplifies to

$$\text{cap}(C') = \frac{\ell(\gamma)}{\pi - 2 \arcsin((\cosh(a_1))^{-1})}. \quad (3)$$

The estimate worsens, if the variation of the boundary,  $\int_{t=0}^{\ell(\gamma)} |a'_1(t)|^2 + |a'_2(t)|^2 dt$  increases.

## 2.2 Hyperbolic trigonometry

Hyperbolic trigonometry is a basic tool in Section 4 of this paper. We will give here the formulas of the polygons used in the following sections:

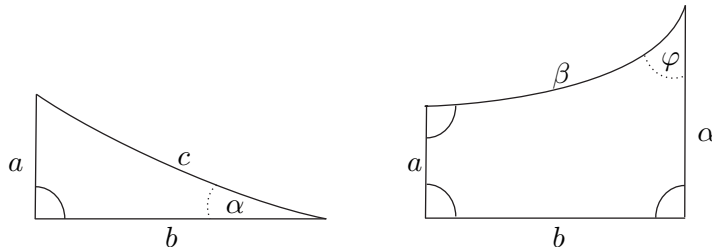


Figure 1: Right-angled triangle and trirectangle

### 1.) Right-angled triangles

$$\begin{aligned} \cosh(\ell(c)) &= \cosh(\ell(a)) \cosh(\ell(b)) \\ \cos(\alpha) &= \tanh(\ell(b)) \coth(\ell(c)) \quad \text{and} \quad \sinh(\ell(a)) = \sin(\alpha) \sinh(\ell(c)) \end{aligned}$$

### 2.) Trirectangles

$$\cosh(\ell(a)) = \tanh(\ell(\beta)) \coth(\ell(b)) \quad \text{and} \quad \sinh(\ell(\alpha)) = \sinh(\ell(a)) \cosh(\ell(\beta))$$

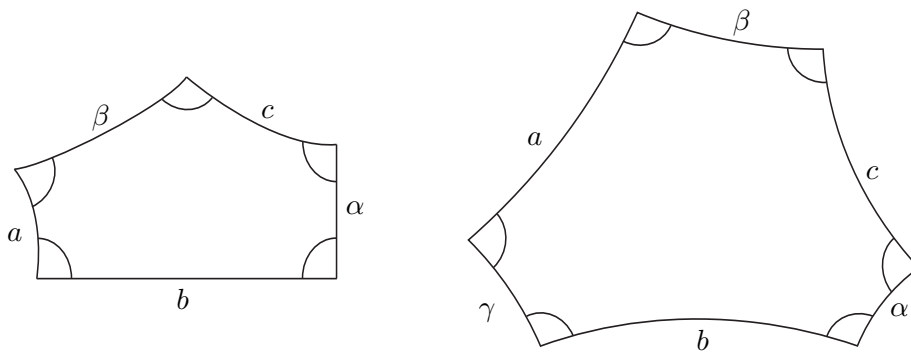


Figure 2: Right-angled pentagon and hexagon

### 3.) Right-angled pentagons

$$\cosh(\ell(c)) = \sinh(\ell(a)) \sinh(\ell(b)) \quad \text{and} \quad \cosh(\ell(c)) = \coth(\ell(\alpha)) \coth(\ell(\beta))$$

### 4.) Right-angled hexagons

$$\cosh(\ell(c)) = \sinh(\ell(a)) \sinh(\ell(b)) \cosh(\ell(\gamma)) - \cosh(\ell(a)) \cosh(\ell(b))$$

### 2.3 Y-pieces and Fenchel-Nielsen coordinates

An important class of hyperbolic Riemann surfaces with geodesic boundary are the surfaces of signature  $(0, 3)$ , or *Y-pieces*. Any Riemann surface of signature  $(g, n)$  can be decomposed into or built from these basic building blocks.

The geometry of a hyperbolic Y-piece is determined by the length of its three boundary geodesics. If  $\mathcal{Y}$  is a Y-piece with boundary geodesics  $\gamma_1, \gamma_2, \gamma_3$ , then we can introduce a marking on  $\mathcal{Y}$ . The marking entails labelling the boundary components to obtain the *marked Y-piece*  $\mathcal{Y}[\gamma_1, \gamma_2, \gamma_3]$ . For  $\mathcal{Y}[\gamma_1, \gamma_2, \gamma_3]$ , we introduce a standard parametrization of the boundaries as explained below. Let  $c_{ij}$  be the geodesic arc going from  $\gamma_i$  to  $\gamma_j$  that meets these boundaries perpendicularly. We set  $\mathbb{S}^1 = \mathbb{R} \text{ mod } (t \mapsto t + 1)$  and parametrize all boundary geodesics

$$\gamma_i : \mathbb{S}^1 \rightarrow \mathcal{Y}[\gamma_1, \gamma_2, \gamma_3], \gamma_i : t \mapsto \gamma_i(t),$$

such that each geodesic is traversed once and with the same orientation. We parametrize the geodesics, such that  $\gamma_1(0)$  is the endpoint of  $c_{31}$ ,  $\gamma_2(0)$  is the endpoint of  $c_{12}$ , and  $\gamma_3(0)$  is the endpoint of  $c_{23}$  (see *Figure 3*).

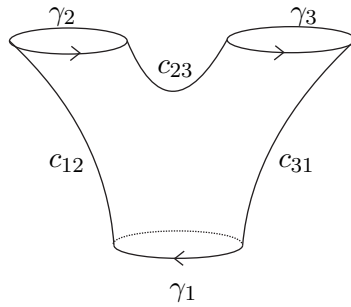


Figure 3: A marked Y-piece  $\mathcal{Y}[\gamma_1, \gamma_2, \gamma_3]$

Two marked Y-pieces  $\mathcal{Y}$  and  $\mathcal{Y}'$ , that have a boundary geodesic of the same length, can be pasted together. If  $\gamma_1 \subset \mathcal{Y}$  and  $\gamma'_1 \subset \mathcal{Y}'$  are the geodesics of equal length, then we can glue  $\mathcal{Y}$  and  $\mathcal{Y}'$  using the identification

$$\gamma_1(t) = \gamma'_1(-t + tw), t \in \mathbb{S}^1,$$

where  $tw \in (-\frac{1}{2}, \frac{1}{2}]$  is an additional constant, called the *twist parameter*. We obtain the surface

$$\mathcal{Y} + \mathcal{Y}' \text{ mod } (\gamma_1(t) = \gamma'_1(-t + tw), t \in \mathbb{S}^1).$$

If  $\gamma$  is the simple closed geodesic in  $\mathcal{Y} + \mathcal{Y}'$ , which corresponds to  $\gamma_1$  in  $\mathcal{Y}$ , then we call  $tw$  the twist parameter at  $\gamma$ .

Every Riemann surface  $S$  of signature  $(g, n)$  can be built from  $2g - 2 + n$  Y-pieces. The pasting scheme can be encoded in a graph  $G(S)$  (see [Bu], pp. 27 -30).

Let  $L(S)$  be the set of  $3g - 3 + n$  lengths of simple closed geodesics in the surface  $S$ , corresponding to the boundary geodesics of the Y-pieces from the construction. Let  $A(S)$  be the set of  $3g - 3 + n$  twist parameters that define the gluing of these geodesics. Then, any Riemann surface  $S$  can be constructed from the information provided in the triplet  $(G(S), L(S), A(S))$ .

**Definition 2.2.**  $(L(S), A(S))$  is the sequence of Fenchel-Nielsen coordinates of the Riemann surface  $S$ .

### 3 Theoretical estimates for the period Gram matrix

Let  $S$  be a Riemann surface of genus  $g \geq 2$ ,  $A$  a canonical basis, and  $P_S$  the period Gram matrix of  $S$  with respect to  $A$ ,

$$P_S = (p_{ij})_{i,j=1,\dots,2g} = \left( \int_S \sigma_i \wedge {}^* \sigma_j \right)_{i,j=1,\dots,2g}.$$

Here we first show how to obtain bounds on the diagonal entries of  $P_S$  using the geometry of embedded cylinders around the elements of the canonical basis. This approach can be elaborated to obtain estimates for all entries of  $P_S$ . It relies on the premise that the cut locus of a given simple closed geodesic on a Riemann surface can be (at least partially) calculated.

#### 3.1 Estimates for the diagonal entries of $P_S$

Let  $T(\alpha_{\tau(i)}) \subset S$  be a topological tube which is obtained by a continuous deformation of a small embedded cylinder  $C(\alpha_{\tau(i)})$  in  $S$  of constant width. We will see in Section 3.1.1 that the capacity of such a tube gives an upper bound for the energy of  $\sigma_i$ ,  $E(\sigma_i) = p_{ii}$ . Consider without loss of generality  $E(\sigma_1) = p_{11}$ .

We will use the tube obtained by cutting open  $S$  along the cut locus  $CL(\alpha_2)$  of  $\alpha_2$ . The *cut locus* of a subset  $X \subset S$ ,  $CL(X)$  is defined as follows:

$$CL(X) := \{y \in S \mid \exists \gamma_{x,y}, \gamma_{x',y}, \gamma_{x,y} \neq \gamma_{x',y}, \text{ with } x, x' \in X \text{ and } \text{dist}(x, y) = \ell(\gamma_{x,y}) = \ell(\gamma_{x',y})\}, \quad (4)$$

where  $\gamma_{a,b}$  denotes a geodesic arc connecting the points  $a$  and  $b$ . We denote by  $S_X$  the surface, which we obtain by cutting open  $S$  along  $CL(X)$ . For a set  $X \subset S$ , set

$$Z_r(X) = \{x \in S \mid \text{dist}(x, X) \leq r\}. \quad (5)$$

If  $U$  is a union of disjoint simple closed geodesics  $(\gamma_i)_{i=1,\dots,n}$ , then for a sufficiently small  $r$ ,  $Z_r(U)$  consists of disjoint cylinders around these geodesics. We obtain  $CL(U)$  by letting  $r$  grow continuously until  $Z_r(U)$  self-intersects. We stop the expansion at the points of intersection, but continue expanding the rest of the set, until the process halts. The points of intersection then form  $CL(U)$ . It follows from this process that the surface  $S_U$ , that we obtain by cutting open  $S$  along  $CL(U)$ , can be retracted onto the union of small cylinders around  $(\gamma_i)_{i=1,\dots,n}$ . If  $U = \gamma$ , then  $S_U$  can be embedded into an sufficiently large cylinder  $C$  around  $\gamma$ . For more information about the cut locus, see [Ba].

Consider an embedding of  $S_{\alpha_2} = S_2$  in a cylinder  $C$  (see *Figure 4*), which, by abuse of notation, we also call  $S_2$ . The boundary  $\partial S_2$  of  $S_2 \subset C$  consists of the two connected components  $\partial_1 S_2$  and  $\partial_2 S_2$ , which are piecewise geodesic (see [Ba]). Fixing a base point  $x \in S_2 \subset C$ , we can construct a primitive  $F_1$  of  $\sigma_1$  by integrating  $\sigma_1$  along paths starting from the base point  $x$ . As  $\int_{\alpha_2} \sigma_1 = 0$ , the value of the integral is independent of the chosen path in  $S_2$ . Hence, there exists

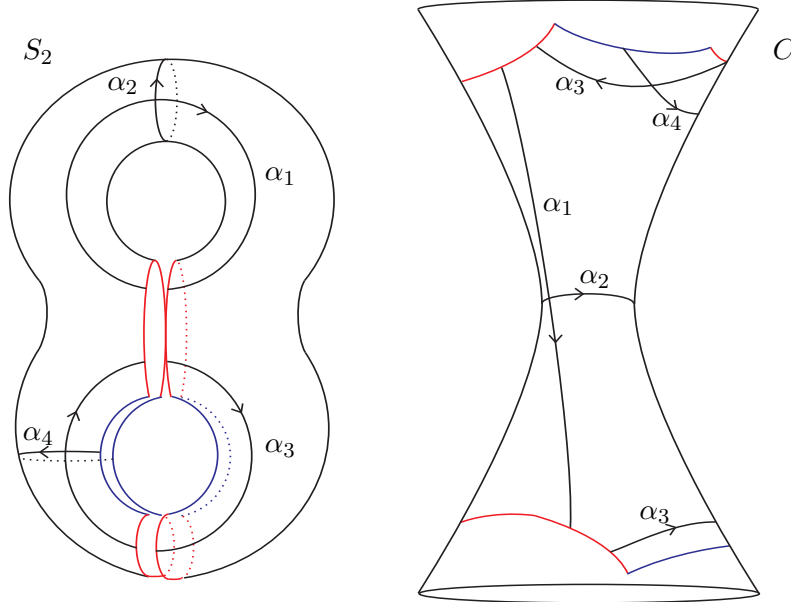


Figure 4: Embedding of  $S_2 = S_{\alpha_2}$  in a cylinder around  $\alpha_2$

a primitive  $F_1$  of  $\sigma_1$  on  $S_2 \subset C$ . Furthermore,  $F_1$  is a real harmonic function, as  $\sigma_1$  is a real harmonic 1-form. We recall that the value of the integral of  $\sigma_1$  over a closed curve depends only on the homology class of the curve. In particular, the value of the integral is the same for two curves in the same free homotopy class.

The conditions on the canonical basis  $A$  imply the following boundary conditions for  $F_1$ . For each point  $p_1$  on the boundary  $\partial S_2 \subset C$ , there exists a point  $p_2$ , such that  $p_1$  and  $p_2$  map to the same point  $p$  on  $S$ , and

$$F_1(p_2) - F_1(p_1) = 0 \quad \text{or} \quad F_1(p_2) - F_1(p_1) = 1.$$

We color  $p_1$  and  $p_2$  blue in the first case and red in the second case and call such a decomposition a *red-blue decomposition* of the cut locus (see *Figure 4*).

Let  $CL^{blue}(\alpha_2)$  and  $CL^{red}(\alpha_2)$  denote the blue and the red parts of  $CL(\alpha_2)$ , both in  $S$  and  $S_2$ . Then

$$CL(\alpha_2) = CL^{blue}(\alpha_2) \cup CL^{red}(\alpha_2).$$

For the red-blue decomposition that is obtained via the cut locus  $CL(\alpha_2)$ , the following holds. If  $p_1$  and  $p_2$  are blue, then  $p_1$  and  $p_2$  lie on the same side of the boundary  $\partial S_2$ . If  $p_1$  and  $p_2$  are red, then they lie on different sides of  $\partial S_2$ . This follows from the relationship of the canonical 1-forms with the intersection number of curves (see [FK], chapter III). At the intersection of the red and the blue parts of a boundary, there exist a finite number points that are both red and blue.

We now connect the endpoints of two corresponding opposite red boundary segments in the red-blue decomposition of  $S_2 \subset C$  with differentiable curves, such that these curves do not mutually intersect. Then the curves, together with the boundary segments of  $S_2$ , enclose a subset of  $S_2$ . Let  $S_2^{red}$  denote the union of all enclosed areas that can be obtained this way.

### 3.1.1 Upper bound

Let  $T(\alpha_2) \subset S$  be a topological tube (with piecewise smooth boundary) which is obtained by a continuous deformation of a small embedded cylinder  $C(\alpha_2)$  with baseline  $\alpha_2$ .

Let  $\tilde{\sigma}_1$  be a closed 1-form that satisfies

$$\int_{[\alpha_k]} \tilde{\sigma}_1 = \delta_{1k} \quad \text{for all } k \in \{1, \dots, 2g\}. \quad (6)$$

Then  $\sigma_1$  is the unique energy-minimizing closed 1-form satisfying the above equation. Hence,  $E(\sigma_1) \leq E(\tilde{\sigma}_1)$ .

Let  $F$  be a function, that solves the capacity problem for  $T(\alpha_2)$ , i.e.

$$F|_{\partial_1 T(\alpha_2)} = 0 \quad , \quad F|_{\partial_2 T(\alpha_2)} = 1 \quad \text{and} \quad \text{cap}(T(\alpha_2)) = E(F).$$

We can smoothen  $F$  in an  $\epsilon$ -environment  $U \subset T(\alpha_2)$  of the boundary of  $T(\alpha_2)$ , to obtain a differentiable function  $F'_1$  on  $T(\alpha_2)$  that satisfies:

There are open subsets  $U_1 \supset \partial_1 T(\alpha_2)$  and  $U_2 \supset \partial_2 T(\alpha_2)$  of  $U$ , such that

$$F'_1|_{U_1} = 0, F'_1|_{U_2} = 1 \quad \text{and} \quad E(F'_1) - \epsilon = E(F) = \text{cap}(T(\alpha_2)),$$

where  $\epsilon > 0$  is a positive real number which can be chosen arbitrarily close to zero. We obtain a closed 1-form  $\sigma'_1$  setting

$$\sigma'_1 = \begin{cases} 0 & \text{on } S \setminus \{T(\alpha_2)\} \\ dF'_1 & \text{on } T(\alpha_2) \end{cases}.$$

Now, due to Stokes theorem,  $\sigma'_1$  is closed 1-form, that satisfies Equation (6). Hence

$$E(\sigma_1) \leq E(\sigma'_1) = \text{cap}(T(\alpha_2)) + \epsilon,$$

The above inequality is also used in [BS], where  $T(\alpha_2) = C(\alpha_2)$  is an embedded cylinder, but the method is not explicitly described there.

Setting  $T(\alpha_2) = S_2$ , we obtain that the capacity  $\text{cap}(S_2)$  of  $S_2 \subset C$  provides an upper bound on the energy of  $\sigma_1$ . We obtain an upper bound on  $\text{cap}(S_2)$  by evaluating the energy of any test function  $F_{1t}$ , that is a Lipschitz function on  $S_2$  and satisfies the boundary conditions of the capacity problem (see [GT]). As  $S_2 \subset C$  is an annulus that satisfies the conditions of **Theorem 2.1**, such a function  $F_{1t}$  is provided there:

$$E(F_{1t}) \geq \text{cap}(S_2) \geq E(\sigma_1) = p_{11}. \quad (7)$$

### 3.1.2 Lower bound

We obtain a lower bound on  $p_{11} = E(F_1)$  as explained next. Consider the set  $S_2^{red}$ . Remember that in each connected subset of  $S_2^{red}$  there are boundary points  $p_1$  and  $p_2$  on opposite sides, such that  $F_1(p_2) - F_1(p_1) = 1$ . We get:

$$E(\sigma_1) = E(F_1) \geq \int_{S_2^{red}} \|DF_1\|_2^2.$$

Let  $I$  be a disjoint union of intervals in  $\mathbb{R}$  and

$$\varphi : I \times [a_1, a_2] \rightarrow S_2^{red}, \varphi : (t, s) \mapsto \varphi(t, s)$$

a bijective function that parametrizes  $S_2^{red}$  as follows:

$$\varphi(I \times \{a_1\}) = S_2^{red} \cap \partial_1 S_2 \quad \text{and} \quad \varphi(I \times \{a_2\}) = S_2^{red} \cap \partial_2 S_2$$

and for a fixed  $c \in I$ ,  $\varphi(\{c\} \times [a_1, a_2])$  is a differentiable curve in  $S_2^{red}$ , such that

$$F_1(\varphi(c, a_2)) - F_1(\varphi(c, a_1)) = 1.$$

Denote by  $\mathcal{F}_1$  the set of functions

$$\mathcal{F}_1 = \{f : S_2^{red} \rightarrow \mathbb{R} \mid f \in \text{Lip}(S_2^{red}) \text{ and } f(\varphi(c, a_2)) - f(\varphi(c, a_1)) = 1 \ \forall \ c \in I\}.$$

We can obtain a lower bound on  $p_{11} = E(\sigma_1) = E(F_1)$  if we find a function  $\tilde{f}_1$ , such that

$$\int_{S_2^{red}} \|D\tilde{f}_1\|_2^2 = \min_{f \in \mathcal{F}_1} \int_{S_2^{red}} \|Df\|_2^2. \quad (8)$$

We call this problem the *free boundary problem* for  $S_2^{red}$ .

Though this problem is quite interesting in its own right, we could not find an explicit solution. To obtain an explicit result, we construct another lower bound based on projection of tangent vectors on curves. For a  $x = \varphi(c, a) \in S_2^{red}$  denote by  $p_\varphi : T_x(S_2^{red}) \rightarrow \{\lambda \cdot \frac{\partial \varphi(c, a)}{\partial s} \mid \lambda \in \mathbb{R}\}$  the orthogonal projection of a tangent vector in  $x$  onto the subspace spanned by  $\frac{\partial \varphi(c, a)}{\partial s}$ . Then we have:

$$E(F_1) \geq \int_{S_2^{red}} \|DF_1\|_2^2 \geq \int_{S_2^{red}} \|p_\varphi(DF_1)\|_2^2 \geq \min_{f \in \mathcal{F}_1} \int_{S_2^{red}} \|p_\varphi(Df)\|_2^2 = \int_{S_2^{red}} \|p_\varphi(Df_1)\|_2^2. \quad (9)$$

Here,  $f_1$  is a function that realizes the minimum. We have  $\int_{S_2^{red}} \|DF_1\|_2^2 = \int_{S_2^{red}} \|p_\varphi(DF_1)\|_2^2$ , if

and only if in every point  $\varphi(t, s) = x \in S_2^{red}$ ,  $\varphi(t, \cdot)$  is orthogonal to the level set of  $F_1$  passing through  $x$ . Note that the problem of finding the function  $f_1$  is in general easier than finding the function  $F_1$  or  $\tilde{f}_1$ . We will apply these ideas to Q-pieces in Section 4. To this end we will use results from the calculus of variations.

Summarizing the inequalities (7)-(9), we obtain the following estimates for  $p_{11} = E(\sigma_1)$ :

$$E(F_{1t}) \geq \text{cap}(S_{\alpha_2}) \geq E(\sigma_1) = E(F_1) \geq \min_{f \in \mathcal{F}_1} \int_{S_2^{red}} \|Df\|_2^2 \geq \min_{f \in \mathcal{F}_1} \int_{S_2^{red}} \|p_\varphi(Df)\|_2^2. \quad (10)$$

Note that the upper bound differs from the lower bound. One reason for this difference is that the test function whose energy provides our upper bound has positive energy on  $S_2 \setminus S_2^{red}$ , whereas the energy is zero in the estimate providing the lower bound. Another difference is due to the use of the projection along lines in the construction of the lower bound. In Section 4, we will apply these methods to a decomposition of the Riemann surface, where the elements of the canonical basis are contained in Q-pieces. There, we will see these two effects explicitly.

### 3.2 Estimates for the non-diagonal entries of $P_S$

We now show, how we can estimate the remaining entries of the period Gram matrix  $P_S$ . Since  $\int_S \cdot \wedge^* \cdot$  is a scalar product, for  $i \neq j$  we have:

$$|p_{ij}| \leq \frac{1}{2} (E(\sigma_i) + E(\sigma_j)), \quad (11)$$

$$p_{ij} = \frac{1}{2} (E(\sigma_i + \sigma_j) - E(\sigma_i) - E(\sigma_j)), \quad \text{and} \quad (12)$$

$$p_{ij} = \frac{1}{2} (E(\sigma_i) + E(\sigma_j) - E(\sigma_i - \sigma_j)). \quad (13)$$

We have shown how to find upper and lower bounds on  $E(\sigma_i)$  and  $E(\sigma_j)$ . We obtain a direct estimate of  $p_{ij}$  from inequality (11). However, to obtain a sharp estimate, both  $E(\sigma_i)$  and  $E(\sigma_j)$  must be small. We will show how to obtain better estimates of  $p_{ij}$  from the following two equations. If we can find upper and lower bounds on either  $E(\sigma_i + \sigma_j)$  or  $E(\sigma_i - \sigma_j)$ , we will obtain an estimate for  $p_{ij}$ .

Now  $\sigma_i + \sigma_j$  and  $\sigma_i - \sigma_j$  satisfy the following equations on the cycles:

$$\int_{[\alpha_k]} \sigma_i + \sigma_j = \delta_{ik} + \delta_{jk} \quad \text{and} \quad \int_{[\alpha_k]} \sigma_i - \sigma_j = \delta_{ik} - \delta_{jk} \quad \text{for all } k \in \{1, \dots, 2g\}. \quad (14)$$

There is a geodesic  $\alpha$  in the homotopy class of either  $\alpha_{\tau(i)} \cdot \alpha_{\tau(j)}$  or  $\alpha_{\tau(i)}(\alpha_{\tau(j)})^{-1}$  which is a simple closed curve. Applying a base change of the canonical basis, we can incorporate  $\alpha$  into a new basis. This can be done, such that one of the two 1-forms  $\sigma_i + \sigma_j$  and  $\sigma_i - \sigma_j$  becomes an element of the new dual basis. Hence we can obtain upper and lower bounds for the energy of one of these harmonic forms using the methods from the previous subsection.

Since it is often difficult to find  $\alpha$ , we will present this approach only for the case  $\alpha_j = \alpha_{\tau(i)}$ . We present these estimates in Section 3.2.1. If  $\alpha_j \neq \alpha_{\tau(i)}$ , we will present an alternative approach in Section 3.2.2. We will make use of both methods in Section 4.

#### 3.2.1 Estimates for a non-diagonal entry $p_{i\tau(i)}$

Consider without loss of generality  $p_{12}$ . Let  $\alpha_{12}$  be the simple closed geodesic in the free homotopy class of  $\alpha_1 \alpha_2^{-1}$ . We apply the base change

$$A = (\alpha_1, \alpha_2, \dots, \alpha_{2g}) \rightarrow (\alpha_{12}, \alpha_2, \dots, \alpha_{2g}) = A'.$$

This way we obtain the dual basis  $(\sigma'_k)_{k=1, \dots, 2g}$  for  $A'$ , where

$$(\sigma_1, \sigma_1 + \sigma_2, \sigma_3, \dots, \sigma_{2g}) = (\sigma'_1, \sigma'_2, \sigma'_3, \dots, \sigma'_{2g}).$$

Let  $F_{12} = F'_2$  be a primitive of  $\sigma_1 + \sigma_2 = \sigma'_2$  on  $S_{\alpha_{12}} = S_{12}$ . We embed  $S_{12}$  into a cylinder  $C$  and denote this surface also by  $S_{12}$ . Proceeding as in the previous subsection, we obtain upper and lower bounds on  $E(\sigma_1 + \sigma_2) = E(\sigma'_2)$  from the geometry of  $S_{12}$ :

$$E(F_{12t}) \geq \text{cap}(S_{12}) \geq E(\sigma_1 + \sigma_2) \geq E_{S_{12}^{\text{red}}}(p_\varphi(Df_{12})).$$

Here  $F_{12t}$  is the test function provided by **Theorem 2.1**, whose energy provides an upper bound for  $\text{cap}(S_{12})$  and  $f_{12}$  is the function constructed analogously to  $f_1$  (see inequality (9)).

Substituting the estimates of  $E(\sigma_1 + \sigma_2)$ ,  $E(\sigma_1)$ , and  $E(\sigma_2)$  in Equation (12), we obtain an upper and lower bound on  $p_{12}$ .

### 3.2.2 Estimates for a non-diagonal entry $p_{ij}$ , where $j \neq \tau(i)$

In this case  $\alpha_i$  and  $\alpha_j$  do not intersect. Consider without loss of generality  $p_{13}$ . For  $\alpha_{\tau(1)} = \alpha_2$  and  $\alpha_{\tau(3)} = \alpha_4$  consider  $S_{\alpha_2 \cup \alpha_4} = S_{24}$ .  $S_{24}$  consists out of two connected parts. Let  $S_{24}^1 \subset S_{\alpha_2}$  be the part that contains  $\alpha_2$  and let  $S_{24}^3 \subset S_{\alpha_4}$  be the part that contains  $\alpha_4$ . We embed  $S_{24}^1$  into a cylinder  $C_1$  around  $\alpha_2$  and  $S_{24}^3$  into a cylinder  $C_3$  around  $\alpha_4$ , and denote the embedded surfaces by the same name. Due to the relationships in Equation (14),  $\sigma_1 + \sigma_3$  has a primitive on both  $S_{24}^1 \subset C_1$  and  $S_{24}^3 \subset C_3$ . Such a decomposition is shown in *Figure 5*.

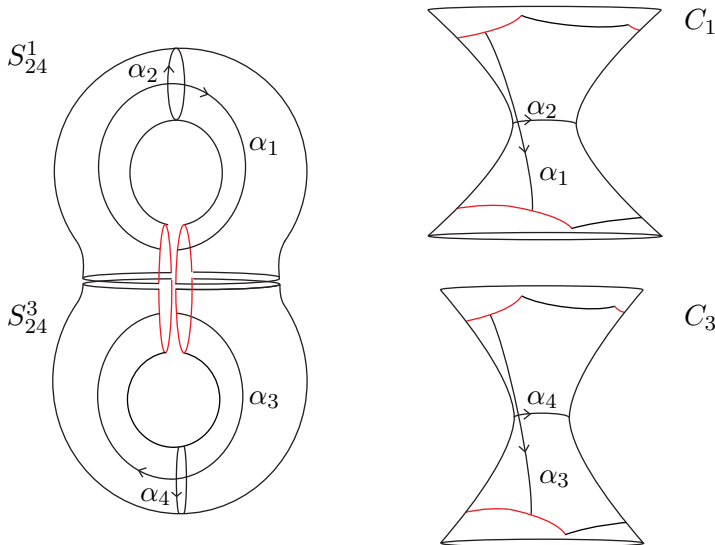


Figure 5: Embedding of  $S_{24}^i$  in a cylinder  $C_i$  around  $\alpha_{\tau(i)}$  for  $i \in \{1, 3\}$

For  $i \in \{1, 3\}$ , let  $\tilde{F}_i$  on  $S_{24}^i$  be a function that satisfies boundary conditions for the capacity problem on  $S_{24}^i$ . Together, these functions naturally define a function  $\tilde{F}_{13}$  on  $S_{24}$ . By smoothing  $\tilde{F}_{13}$  in an inner environment of the boundary of  $S_{24}$ , we obtain a function  $f_{13}$  on  $S$ , whose derivative  $df_{13}$  is a closed differential form that satisfies the same integral conditions on the cycles as  $\sigma_1 + \sigma_3$ . Due to the energy-minimizing property of  $\sigma_1 + \sigma_3$ ,  $E(\tilde{f}_{13}) \geq E(\sigma_1 + \sigma_3)$ . Hence, the sum of the capacities of  $S_{24}^1$  and  $S_{24}^3$  provides an upper bound for  $E(\sigma_1 + \sigma_3)$ :

$$\text{cap}(S_{24}^1) + \text{cap}(S_{24}^3) \geq E(\sigma_1 + \sigma_3).$$

We obtain a lower bound for  $E(\sigma_1 + \sigma_3)$  by applying the same methods used to obtain a lower bound on  $E(\sigma_1)$  on  $S_2$  (see Section 3.1.2). Below, we obtain estimates from the red-blue decompositions induced by a primitive  $F_{13}$  of  $\sigma_1 + \sigma_3$  on the boundary of  $S_{24}^1$  in  $C_1$  and  $S_{24}^3$  in  $C_3$ . The only difference is that we have some segments of the boundary, where the red-blue decomposition does not apply. Here we disregard these pieces in the construction of  $S_{24}^{1red}$  and  $S_{24}^{3red}$ . As these sets are disjoint, we need a certain function  $f_{13}$  that satisfies

$$f_{13}(p_2) - f_{13}(p_1) = F_{13}(p_2) - F_{13}(p_1) = 1$$

for all points  $p_1, p_2$  in  $\partial S_{24}^{1red}$  or  $\partial S_{24}^{3red}$ . Let  $p_\varphi$  be the projection of a vector field in the tangent space onto lines of a suitable parametrization  $\varphi$  of  $S_{24}^{1red}$  and  $S_{24}^{3red}$ . Let  $f_{13}$  furthermore be a

function that minimizes the projected energy  $E(p_\varphi(D\cdot))$ . With  $S_{24}^r = S_{24}^{1red} \cup S_{24}^{3red}$ , we have:

$$E(\sigma_1 + \sigma_3) \geq E_{S_{24}^r}(p_\varphi(Df_{13})).$$

Substituting the estimates for  $E(\sigma_1 + \sigma_3)$ ,  $E(\sigma_1)$ , and  $E(\sigma_3)$  in Equation (12), we obtain upper and lower bounds on  $p_{13}$ :

$$p_{13} \leq \frac{1}{2} \left( \text{cap}(S_{24}^1) + \text{cap}(S_{24}^3) - E_{S_{\alpha_2}^{red}}(p_\varphi(Df_1)) - E_{S_{\alpha_4}^{red}}(p_\varphi(Df_3)) \right) > 0 \quad \text{and} \quad (15)$$

$$p_{13} \geq \frac{1}{2} \left( E_{S_{24}^r}(p_\varphi(Df_{13})) - \text{cap}(S_{\alpha_2}) - \text{cap}(S_{\alpha_4}) \right) < 0. \quad (16)$$

In the above equation,  $f_3$  is the minimizing function corresponding to a primitive  $F_3$  of  $\sigma_3$  on  $S_{\alpha_4}^{red}$ , constructed analogously to  $f_1$  in Section 3.1.2 (see inequality (9)). That our estimate for  $p_{13}$  in the first inequality is bigger than zero can be seen as follows. By construction, we have

$$S_{24}^1 \subset S_{\alpha_2} \quad \text{and} \quad S_{24}^3 \subset S_{\alpha_4}.$$

Now, if an annulus  $R_1$  is contained in an annulus  $R_2$ , then  $\text{cap}(R_1) \geq \text{cap}(R_2)$ . Hence

$$\text{cap}(S_{24}^1) \geq \text{cap}(S_{\alpha_2}) > E_{S_{\alpha_2}^{red}}(p_\varphi(Df_1)) \quad \text{and} \quad \text{cap}(S_{24}^3) \geq \text{cap}(S_{\alpha_4}) > E_{S_{\alpha_4}^{red}}(p_\varphi(Df_3)),$$

from which follows the last inequality in (15).

It follows furthermore from the boundary conditions of the functions  $F_1, F_3$ , and  $F_{13}$  that

$$\partial S_{24}^{1red} \subset \partial S_{\alpha_2}^{red} \quad \text{and} \quad \partial S_{24}^{3red} \subset \partial S_{\alpha_4}^{red}.$$

Hence

$$E_{S_{24}^r}(p_\varphi(Df_{13})) = E_{S_{24}^{1red}}(p_\varphi(Df_{13})) + E_{S_{24}^{3red}}(p_\varphi(Df_{13})) \leq E_{S_{\alpha_2}^{red}}(p_\varphi(Df_1)) + E_{S_{\alpha_4}^{red}}(p_\varphi(Df_3)).$$

Now the second inequality in (16) follows from this inequality and the fact that  $E_{S_{\alpha_2}^{red}}(p_\varphi(Df_1)) < \text{cap}(S_{\alpha_2})$  and  $E_{S_{\alpha_4}^{red}}(p_\varphi(Df_3)) < \text{cap}(S_{\alpha_4})$ .

Using this approach, we can only obtain optimal estimates if  $p_{13}$  is close to zero. This is due to the fact that we do not have full information of the boundary values on our tubes  $S_{24}^3$  and  $S_{24}^1$ . This estimate is however better than the one obtained from Equation (11). Note that by **Example 1.3** the value of  $p_{13}$  is close to zero, if  $\alpha_2$  and  $\alpha_4$  are separated by a small separating simple closed geodesic  $\gamma$ .

### 3.3 Examples

We now give two examples to demonstrate the weaknesses and strengths of our method. We first show that the energy of a dual harmonic form can be lower than the capacity of a cylinder of even infinite length. The following example is due to Peter Buser.

**Example 3.1** For comparison we briefly review the example of the necklace surface given in [BSe1]. Let  $\mathcal{Y}$  be a Y-piece, a surface of signature  $(0, 3)$ . Let  $\gamma, \eta$  and  $\eta'$  be its boundary geodesics, such that  $\eta$  and  $\eta'$  have equal length. We paste two copies of  $\mathcal{Y}$  along  $\eta$  and  $\eta'$  to obtain  $\mathcal{R}$  of signature  $(1, 2)$ . As shown in *Figure 6*, the necklace surface  $N$  of genus  $g$  is obtained

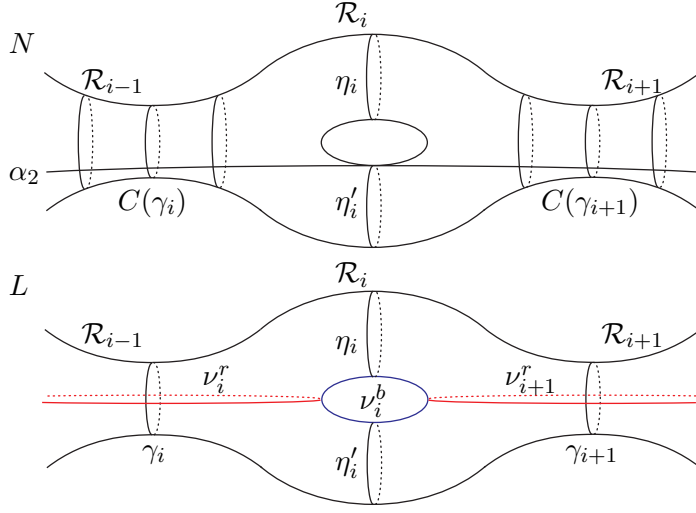


Figure 6: Building blocks for the surfaces  $N$  and  $L$  of genus  $g$

by pasting together  $g - 1$  copies  $\mathcal{R}_1, \dots, \mathcal{R}_{g-1}$  of a building block  $\mathcal{R}$ . The free boundary of  $\mathcal{R}_{g-1}$  is pasted along  $\gamma_1$  of  $\mathcal{R}_1$  to obtain a ring. In this example, the twist parameter for any pasting can be chosen arbitrarily.

By the collar lemma (see [Bu], p. 106), each  $\gamma_i$  has a collar of width  $w_\gamma$ , where

$$w_\gamma \geq \operatorname{arcsinh} \left( \frac{1}{\sinh(\frac{\ell(\gamma)}{2})} \right).$$

Let  $\mathbf{A} = (\alpha_i)_{i=1, \dots, 2g}$  be a canonical basis, such that  $\alpha_1 = \gamma_1$  and  $\alpha_{\tau(1)} = \alpha_2$  is a simple closed geodesic that intersects all  $(\gamma_i)_{i=1, \dots, g-1}$  exactly once. Let  $P_S$  be the corresponding period Gram matrix. We will examine the upper bound on the entry  $p_{22} = E(\sigma_2)$ .

Following our method, we have to embed  $N_1 = N_{\alpha_1}$  into a cylinder  $C_1$  and have to evaluate  $\operatorname{cap}(N_1)$ . Now if an annulus  $R_1$  is contained in an annulus  $R_2$ , then  $\operatorname{cap}(R_1) \geq \operatorname{cap}(R_2)$ , and hence  $\operatorname{cap}(N_1) \geq \operatorname{cap}(C_1)$ . From Equation (3), it follows that the capacity of the cylinder  $C_1$  with baseline of length  $\ell(\alpha_1) = \ell(\gamma)$  of infinite width is not zero. We obtain

$$\operatorname{cap}(N_1) \geq \operatorname{cap}(C_1) = \frac{\ell(\gamma)}{\pi}. \quad (17)$$

We now give another estimate for the energy of  $\sigma_2$  with the help of a test form  $s_2$ . This approach applies only to this example. To this end consider the collar  $C(\gamma_i)$  of a  $\gamma_i$ . On each  $C(\gamma_i)$  set  $s_2 = dF_2$ , where  $F_2$  is the real harmonic function that has value 0 on one boundary of  $C(\gamma_i)$  and  $\frac{1}{g-1}$  on the other. We set  $s_2 = 0$  on  $S \setminus \bigcup_{i=1}^{g-1} C(\gamma_i)$ . Then  $s_2$  is arbitrarily close to a closed form that satisfies the same conditions on the elements of  $\mathbf{A}$  as  $\sigma_2$  and we have

$$E(\sigma_2) < E(s_2) \leq (g-1) \cdot \frac{(g-1)^{-2} \cdot \ell(\gamma)}{\pi - 2 \arcsin \left( \frac{1}{\cosh(w_\gamma)} \right)}, \quad (18)$$

where  $w_\gamma$  is bounded from below by the collar lemma. Summing up the inequalities (17) and (18), we obtain the statement in **Example 1.1**. Hence,  $E(\sigma_2)$  is at most of order  $\frac{1}{g}$  and goes to zero as  $g$  goes to infinity. Our upper bound, on the contrary, is always bigger than the constant  $\frac{\ell(\gamma)}{\pi}$ . This shows that there exist examples where our upper bound can not be of the right order. This might be due to the fact that the projection of  $CL^{blue}(\alpha_1)$  onto  $\alpha_1$  can attain almost the length of  $\alpha_1$ . Hence, as  $CL^{blue}(\alpha_1)$  is large,  $E(\sigma_2)$  might be small.

**Example 3.2** For our second example we construct a linear surface  $L$  of genus  $g$ . This example belongs to the class of M-curves described in [BSi]. In this construction, we use Y-pieces  $\mathcal{Y}$ , where the length of  $\eta$  and  $\eta'$  is large. We construct  $\mathcal{R}$  from two copies of these Y-pieces as in the previous example, however, here the twist parameter in the two pastings is zero. To construct a surface  $L$  of genus  $g$ , we paste together  $g - 2$  copies  $\mathcal{R}_2, \dots, \mathcal{R}_{g-1}$  along the  $\gamma_i$  (see *Figure 6*). Then, we take two copies of  $\mathcal{Y}$ ,  $\mathcal{Y}_1$ , and  $\mathcal{Y}_g$  and paste each together along  $\eta$  and  $\eta'$  to obtain  $\mathcal{Q}_1$ , and  $\mathcal{Q}_g$ , respectively. For  $i \in \{1, g\}$ , let  $\eta_i$  denote the image of  $\eta$  in  $\mathcal{Q}_i$ . Then we paste  $\mathcal{Q}_1$  and  $\mathcal{Q}_g$  on each side of  $\mathcal{R}_2$  and  $\mathcal{R}_{g-1}$ , respectively. Again, the twist parameter for any pasting is zero.

Let  $A = (\alpha_i)_{i=1, \dots, 2g}$  be a canonical basis, such that  $\alpha_1 = \eta_1$  and  $\alpha_2$  is the unique simple closed geodesic in  $\mathcal{Q}_1$  that intersects  $\alpha_1$  perpendicularly. Let  $P_L$  be the corresponding period matrix. We now show that in this case, the upper bound for  $p_{22} = E(\sigma_2)$  is optimal. Therefore we use the symmetries of the surface  $L$ .

To this end, we first determine the cut locus  $CL(\alpha_1)$  of  $\alpha_1$ . For  $i \in \{2, \dots, g\}$  let  $\nu_i^r$  be the simple closed geodesic that intersects the geodesic  $\gamma_i$  perpendicularly. Set  $\nu_1^b = \alpha_2$  and for  $i \in \{2, \dots, g - 1\}$  let  $\nu_i^b \subset \mathcal{R}_i$  be the simple closed geodesic that intersect  $\eta_i$  and  $\eta'_i$  perpendicularly (see *Figure 6*). Set  $\nu_{g+1}^r = \eta_g$  and let  $\nu_g^b$  be the simple closed geodesic intersecting  $\eta_g$  perpendicularly. We make the following claim:

**Claim.** *The cut locus  $CL(\alpha_1) = CL(\alpha_1)^{red} \cup CL(\alpha_1)^{blue}$  of  $\alpha_1$  in  $L$  consists of the sets*

$$CL(\alpha_1)^{red} = \{\nu_2^r, \dots, \nu_{g+1}^r\} \quad \text{and} \quad CL(\alpha_1)^{blue} = \{\nu_2^b, \dots, \nu_g^b\}.$$

*Proof.* Set

$$CL_1 = \{\nu_2^r, \dots, \nu_{g+1}^r\} \cup \{\nu_2^b, \dots, \nu_g^b\}.$$

We have to show that  $CL_1$  is indeed  $CL(\alpha_1)$ . To this end, we show that for any point  $q$  in  $L \setminus \{CL_1\}$  there exists exactly one geodesic arc realizing the distance between  $q$  and  $\alpha_1$ . It follows from the definition of the cut locus (see (4)), that  $q$  does not belong to  $CL(\alpha_1)$ . Hence  $CL(\alpha_1) \subset CL_1$ . We recall that cutting  $L$  along  $CL(\alpha_1)$  we obtain a tube. Now cutting  $L$  along  $CL_1$  we obtain a topological tube and if only if we cut along all points of  $CL_1$ . Hence it follows that  $CL_1 = CL(\alpha_1)$ . The decomposition of  $CL(\alpha_1)$  into  $CL(\alpha_1)^{red}$  and  $CL(\alpha_1)^{blue}$  then follows from the definition of the red-blue decomposition of  $CL(\alpha_1)$ .

Let  $q$  be a point in  $L \setminus \{CL_1 \cup \nu_1^b\}$ . We first show that any geodesic arc realizing the distance  $\text{dist}(q, \alpha_1)$  between  $q$  and  $\alpha_1$  does not intersect  $\{CL_1 \cup \nu_1^b\}$ . To this end we make use of the isometries of  $L$ .

- Let  $\phi_1 \in \text{Isom}(L)$  be the hyperelliptic involution that fixes  $CL_1$  as a set, such that for all  $i \in \{2, \dots, g - 1\}$ :  $\phi_1(\eta_i) = \eta'_i$ .
- Let  $\phi_2 \in \text{Isom}(L)$  be the isometry that fixes  $CL_1$  as a set and all  $\nu_i^b$  point-wise.

- Set  $\phi = \phi_1 \circ \phi_2$ .

Now assume that there is a geodesic arc  $\delta$ , such that

$$\text{dist}(q, \alpha_1) = \ell(\delta),$$

with  $\delta$  intersecting  $\{CL_1 \cup \nu_1^b\}$  transversally. We consider two cases - either  $\delta$  intersects one of the  $(\nu_i^b)_{i=1, \dots, g}$  or  $\delta$  intersects one of the  $(\nu_i^r)_{i=2, \dots, g+1}$ .

In the first case, we assume that  $\delta$  intersects without loss of generality  $\nu_1^b$  in a point  $s$ . Now,  $s$  divides  $\delta$  into two arcs,  $\delta^1$  connecting  $\alpha_1$  and  $s$  and  $\delta^2$  connecting  $s$  with  $q$ . Consider the point  $\phi_2(q)$  and the geodesic arc  $\phi_2(\delta)$ . Since  $\phi_2(\alpha_1) = \alpha_1$ , this is a geodesic arc, such that

$$\ell(\phi_2(\delta)) = \text{dist}(\phi_2(q), \phi_2(\alpha_1)) = \text{dist}(\phi_2(q), \alpha_1) = \ell(\delta).$$

Since  $\phi_2(s) = s$ , the curve  $d = \phi_2(\delta^1) \cup \delta^2$  connects  $\alpha_1$  with  $q$ . Since  $\phi_2$  is an isometry, we have  $\ell(d) = \ell(\delta)$ . But  $d$  intersects the geodesic  $\nu_1^b$  under an angle  $\theta$ . Hence, by applying a small deformation to  $d$ , we can deform  $d$  into a curve  $d'$ , such that

$$\ell(d') < \ell(d) = \ell(\delta) = \text{dist}(q, \alpha_1),$$

which contradicts the definition of  $\delta$ . Hence  $\delta$  does not intersect  $\{CL_1 \cup \nu_1^b\}$ .

If  $\delta$  intersects one of the simple closed geodesic in the set  $(\nu_i^r)_{i=2, \dots, g+1}$  then we obtain a contradiction in a similar fashion. In that case we use the isometry  $\phi$  instead of  $\phi_2$  to obtain our statement.

We now show that for any point in  $L \setminus \{CL_1\}$  there exists exactly one geodesic arc realizing the distance between this point and  $\alpha_1$ , from which follows that  $CL_1 = CL(\alpha_1)$ .

Assume to the contrary and let  $q \in L \setminus \{CL_1\}$  be a point for which there exist two geodesic arcs  $\delta_1$  and  $\delta_2$ , such that

$$\text{dist}(q, \alpha_1) = \ell(\delta_1) = \ell(\delta_2).$$

We first treat the case where  $q \notin \nu_1^b$ . Consider the set  $\{CL_1 \cup \nu_1^b \cup \alpha_1\}$ . This set divides  $L$  into two parts. Let  $L^1$  and  $L^2$  be the surfaces which we obtain by cutting  $L$  along  $CL_1 \cup \nu_1^b \cup \alpha_1$ . Without loss of generality, let  $L^1$  be the surface containing  $q$ .  $L^1$  lifts to a hyperbolic  $4g$ -gon  $\mathcal{P}_{4g}$  in the universal covering. Since all angles at the vertices are  $\frac{\pi}{2}$ ,  $\mathcal{P}_{4g}$  is convex. Let  $\alpha'_1$  be the smooth boundary line of  $\mathcal{P}_{4g}$  that maps to  $\alpha_1$  under the covering map, and let  $q' \in \mathcal{P}_{4g}$  be a lift of  $q$ . Let  $\delta'_1$  and  $\delta'_2$  be a lift of  $\delta_1$  and  $\delta_2$ , respectively, with endpoint  $q'$ . As both  $\delta_1$  and  $\delta_2$  are contained in  $L^1$ ,  $\delta'_1$  and  $\delta'_2$  are contained in  $\mathcal{P}_{4g}$ . Furthermore, since  $\delta_1$  and  $\delta_2$  realize the distance between  $\alpha_1$  and  $q$ , they meet  $\alpha_1$  perpendicularly at their respective endpoints. Hence,  $\delta'_1$  and  $\delta'_2$  meet  $\alpha'_1$  perpendicularly at their endpoints. Let  $\alpha'$  be the arc of  $\alpha'_1$  connecting these two endpoints. Then  $\alpha'$ ,  $\delta'_1$ , and  $\delta'_2$  form a triangle where two interior angles are  $\frac{\pi}{2}$ . But such a triangle does not exist in the hyperbolic plane. This is a contradiction. Hence, for  $q \in L \setminus \{CL_1 \cup \nu_1^b\}$  there is only one geodesic arc in  $L$  realizing the distance between  $q$  and  $\alpha_1$  and therefore  $q \notin CL(\alpha_1)$ .

Now, if  $q \in \nu_1^b$ , it follows from the geometry of  $\mathcal{Q}_1$  that only the intersection point of  $\nu_1^b$  with  $\nu_2^r$  is part of  $CL(\alpha_1)$ . To summarize, we obtain that  $CL_1 = CL(\alpha_1)$ . This settles our claim.  $\square$

We now show that our capacity estimate for  $p_{22} = E(\sigma_2)$  is almost sharp. To this end we consider again the isometries  $\phi_1$ ,  $\phi_2$  and  $\phi$  in  $\text{Isom}(L)$ .  $\phi$  is the isometry that maps any point  $p$  in  $CL(\alpha_1)^{\text{red}} \subset S_1$  to the corresponding point  $p'$  in the red-blue composition induced by  $\sigma_2$ .

Consider now a primitive  $F_2$  of  $\sigma_2$  on  $L_{\alpha_1} = L_1$ .  $F_2 \circ \phi_2$  is a harmonic function, whose derivative

$d(F_2 \circ \phi_2)$  defines a 1-form  $\sigma'_2$  on  $L$ .  $\sigma'_2$  satisfies the same conditions on the cycles as  $\sigma_2$ . Due to the uniqueness of  $\sigma_2$ ,  $\sigma'_2 = \sigma_2$ . In the same way  $1 - F_2 \circ \phi_1$  is a harmonic form, whose derivative  $-d(F_2 \circ \phi_1)$  defines a 1-form  $\sigma''_2$  on  $L$  that satisfies the same integral conditions on the cycles as  $\sigma_2$ . This leads to  $\sigma''_2 = \sigma_2$ . By choosing an appropriate additive constant, we obtain:

$$F_2 \circ \phi_2 = F_2 \quad \text{and} \quad 1 - F_2 \circ \phi_1 = F_2.$$

Now, for any  $p$  on one side of  $CL(\alpha_1)^{red} \subset L_1$ , we have  $F_2(p) - F_2(\phi(p)) = 1$ . Together with the above equation we obtain:

$$F_2(\phi(p)) = 0 \quad \text{and} \quad F_2(p) = 1.$$

Hence, the red parts of the boundary satisfy the conditions for the capacity problem. Consider the two boundary geodesics  $\eta$  and  $\eta'$  of our building block  $\mathcal{Y}$ . If  $\ell(\eta) = \ell(\eta')$  is large, then it follows from hyperbolic geometry that the curves  $(\nu_i^b)_{i=1,\dots,g}$  are arbitrarily small. Hence in this case we obtain

$$p_{22} = E(\sigma_2) = \text{cap}(L_1) - \epsilon_L,$$

where  $\epsilon_L > 0$  depends on the geometry of  $L$  and may become arbitrarily small. Hence our upper bound for a diagonal entry of  $P_L$  is sharp. This is the inequality in **Example 1.2**.

## 4 Estimates for the period Gram matrix based on Q-pieces

In this section we present practical estimates for the period Gram matrix, based on the Fenchel-Nielsen coordinates of Q-pieces containing the paired curves of a canonical basis. Under this condition, the cut loci of these curves can be (at least partially) calculated.

More precisely, let  $S$  be a Riemann surface of genus  $g \geq 2$ . Let  $(\mathcal{Q}_i)_{i=1,3,\dots,2g-1} \subset S$  be a set of Q-pieces, whose interiors are pairwise disjoint. Let  $\beta_i$  be the boundary geodesic of  $\mathcal{Q}_i$ ,  $\alpha_i$  an interior simple closed geodesic, and  $tw_i \in (-\frac{1}{2}, \frac{1}{2}]$  the twist parameter at  $\alpha_i$ . The geometry of  $\mathcal{Q}_i$  is determined by the triplet  $(\ell(\beta_i), \ell(\alpha_i), tw_i)$ .

Now fix an  $i \in \{1, 3, \dots, 2g-1\}$ . Let  $\alpha_{\tau(i)} \subset \mathcal{Q}_i$  be a simple closed geodesic that intersects  $\alpha_i$  exactly once, and  $\alpha_{i\tau(i)} \subset \mathcal{Q}_i$  the simple closed geodesic in the free homotopy class of  $\alpha_i(\alpha_{\tau(i)})^{-1}$ . For  $j \in \{i, \tau(i), i\tau(i)\}$ , let

- $\beta_j = \beta_i$  be the boundary geodesic
- $tw_j$  the twist parameter at  $\alpha_j$
- $FN_j := (\ell(\beta_j), \ell(\alpha_j), tw_j)$  the corresponding Fenchel-Nielsen coordinates of  $\mathcal{Q}_i$ .

In **Lemma 4.2** we show how to find a suitable  $\alpha_{\tau(i)}$  how to calculate  $FN_{\tau(i)}$  and  $FN_{i\tau(i)}$  from  $FN_i$ . This enables us to state estimates for all entries of the period Gram matrix  $P_S$  of  $S$  based on the  $3g$  Fenchel-Nielsen coordinates  $(FN_i)_{i=1,3,\dots,2g-1}$ :

**Theorem 4.1.** *Let  $S$  be a Riemann surface of genus  $g \geq 2$  and  $(\mathcal{Q}_i)_{i=1,3,\dots,2g-1} \subset S$  be a set of Q-pieces, whose interiors do not mutually intersect. If  $\mathcal{Q}_i$  is given in the Fenchel-Nielsen coordinates  $FN_i = (\ell(\beta_i), \ell(\alpha_i), tw_i)$ , where  $\alpha_i$  is an interior simple closed geodesic, such that  $\cosh(\frac{\ell(\alpha_i)}{2}) \leq \cosh(\frac{\ell(\beta_i)}{6}) + \frac{1}{2}$ .*

Then there is a simple closed geodesic  $\alpha_{\tau(i)} \subset \mathcal{Q}_i$ , and a simple closed geodesic  $\alpha_{i\tau(i)}$  in the free homotopy class of  $\alpha_i(\alpha_{\tau(i)})^{-1}$ , and the following functions

$$\begin{aligned} f^u, f^l &: \mathbb{R}^+ \times \mathbb{R}^+ \times \left(-\frac{1}{2}, \frac{1}{2}\right] \rightarrow \mathbb{R}^+ \quad (\text{see Section 4.4}) \\ f^u &: FN_j \mapsto f^u(FN_j) \quad \text{and} \quad f^l : FN_j \mapsto f^l(FN_j), \end{aligned}$$

that provide upper and lower bounds for all entries of the corresponding period Gram matrix  $PS = (p_{ij})_{i,j}$  as follows:

For a diagonal entry  $p_{ii}$ , we have:

$$f^l(FN_{\tau(i)}) \leq p_{ii} \leq f^u(FN_{\tau(i)}).$$

For a non-diagonal entry  $p_{i\tau(i)}$ , we have:

$$\begin{aligned} p_{i,\tau(i)} &\leq \frac{1}{2} \left( f^u(FN_{i\tau(i)}) - f^l(FN_{\tau(i)}) - f^l(FN_i) \right) \quad \text{and} \\ p_{i,\tau(i)} &\geq \frac{1}{2} \left( f^l(FN_{i\tau(i)}) - f^u(FN_{\tau(i)}) - f^u(FN_i) \right). \end{aligned}$$

For a non-diagonal entry  $p_{ik}$ , where  $k \neq \tau(i)$ , we have:

$$0 \leq |p_{i,k}| \leq \frac{1}{2} \left( f^u(FN_{\tau(i)}) + f^u(FN_{\tau(k)}) - f^l(FN_{\tau(i)}) - f^l(FN_{\tau(k)}) \right).$$

The condition on the length  $\ell(\alpha_i)$  of  $\alpha_i$  in **Theorem 4.1** is due to technical reasons. Such a pair  $(\alpha_i, \beta_i)$  always exists by [Pa], **Proposition 5.4**. Though this assumption is not mandatory, it will simplify the calculations in Section 4.1.

In Sections 4.2 and 4.3, we develop the functions  $f^u$  and  $f^l$  explicitly. In Section 4.4, we summarize these formulas and give a summary of our estimates in *Table 1* and *2*. Lastly, we give a good example for our estimates in **Example 4.3**.

#### 4.1 Conversion of Fenchel-Nielsen coordinates for a Q-piece

**Lemma 4.2.** Let  $\mathcal{Q}_1$  be a Q-piece given in the Fenchel-Nielsen coordinates  $(\ell(\beta_1), \ell(\alpha_1), tw_1)$ , where

- $\beta_1$  is the boundary geodesic
- $\alpha_1$  an interior simple closed geodesic, such that  $\cosh\left(\frac{\ell(\alpha_1)}{2}\right) \leq \cosh\left(\frac{\ell(\beta_1)}{6}\right) + \frac{1}{2}$
- $tw_1$  the twist parameter at  $\alpha_1$ .

Then, there is a simple closed geodesic  $\alpha_2 \subset \mathcal{Q}_1$ , and a simple closed geodesic  $\alpha_{12}$  in the free homotopy class of  $\alpha_1(\alpha_2)^{-1}$ , such that

$$\cosh\left(\frac{\ell(\alpha_k)}{2}\right) = \cosh\left(\frac{\ell(\alpha_1)|t'_k|}{2}\right) \sqrt{\left(\frac{\cosh\left(\frac{\ell(\beta_1)}{4}\right)}{\sinh\left(\frac{\ell(\alpha_1)}{2}\right)}\right)^2 + 1}, \quad \text{where } |t'_k| = \begin{cases} |tw_1| & \text{if } k = 2 \\ 1 - |tw_1| & \text{if } k = 12. \end{cases}$$

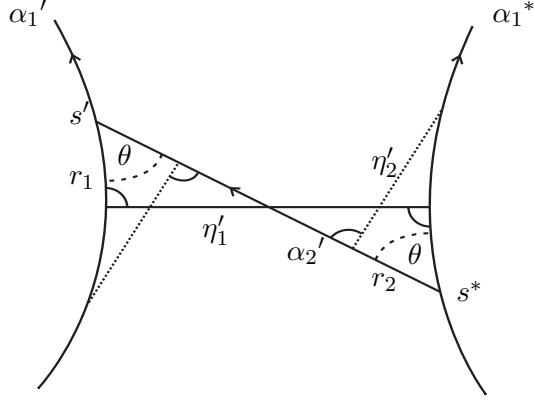


Figure 7: Two lifts of  $\alpha_1$  in the universal covering

Furthermore, for  $k \in \{2, 12\}$ , let  $tw_k$  be the twist parameter at  $\alpha_k$ , then

$$|tw_k| = \min\left\{\frac{2r_k}{\ell(\alpha_k)}, 1 - \frac{2r_k}{\ell(\alpha_k)}\right\}, \quad \text{where } r_k = \operatorname{arctanh}\left(\frac{\tanh\left(\frac{\ell(\alpha_1)|tw_1|}{2}\right) \tanh\left(\frac{\ell(\alpha_1)}{2}\right)}{\tanh\left(\frac{\ell(\alpha_k)}{2}\right)}\right).$$

*Proof.* In  $\mathcal{Q}_1$  there exists a unique shortest geodesic arc  $\eta_1$  meeting  $\alpha_1$  perpendicularly on both sides of  $\alpha_1$ . *Figure 7* shows a lift of  $\alpha_1$  and  $\eta_1$  in the universal covering,  $\alpha_1$  lifts to  $\alpha_1'$  and  $\alpha_1^*$  and  $\eta_1$  to  $\eta_1'$ . Note that  $\alpha_1'$  and  $\alpha_1^*$  have the same orientations with respect to  $\eta_1'$ . In the covering there exist two points,  $s' \in \alpha_1'$  and  $s^* \in \alpha_1^*$ , on opposite sites of  $\eta_1'$  and at the same distance from  $\eta_1'$ , such that  $s'$  and  $s^*$  are mapped to the same point  $s \in \alpha_1$  by the covering map. Observe that  $s'$  and  $s^*$  can always be found, such that the distance  $r_1$  from  $\eta_1'$  is equal to  $\frac{\ell(\alpha_1) \cdot |tw_1|}{2}$ . Let  $\alpha_2'$  denote the geodesic from  $s'$  to  $s^*$ . Using  $\alpha_2'$  we obtain two isometric right-angled geodesic triangles. Since  $\alpha_2'$  intersects  $s'$  and  $s^*$  under the same angle  $\theta$ , the image  $\alpha_2$  of  $\alpha_2'$  under the universal covering map is a smooth simple closed geodesic, which intersects  $\alpha_1$  exactly once. Hence we can incorporate  $\alpha_2$  into our canonical basis for  $S$ . Applying the cosine formula to one of the isometric triangles (see Section 2.2), we obtain:

$$\cosh\left(\frac{\ell(\alpha_2)}{2}\right) = \cosh(r_1) \cosh\left(\frac{\ell(\eta_1)}{2}\right), \quad \text{where } r_1 = \frac{\ell(\alpha_1) \cdot |tw_1|}{2}.$$

The length  $\ell(\eta_1)$  of  $\eta_1$  can be calculated from a decomposition of  $\mathcal{Q}_1$  into a Y-piece (see Equation (20)), leading to

$$\sinh\left(\frac{\ell(\eta_1)}{2}\right) = \frac{\cosh\left(\frac{\ell(\beta_1)}{4}\right)}{\sinh\left(\frac{\ell(\alpha_1)}{2}\right)} \quad \text{thus} \quad \cosh\left(\frac{\ell(\eta_1)}{2}\right) = \sqrt{\left(\frac{\cosh\left(\frac{\ell(\beta_1)}{4}\right)}{\sinh\left(\frac{\ell(\alpha_1)}{2}\right)}\right)^2 + 1}.$$

For further calculations we also need the angle  $\theta$ . From hyperbolic geometry we obtain:

$$\cos(\theta) = \tanh\left(\frac{\ell(\alpha_1) \cdot |tw_1|}{2}\right) \coth\left(\frac{\ell(\alpha_2)}{2}\right) \quad (19)$$

In  $\mathcal{Q}_1$ , there exists likewise a unique shortest geodesic arc  $\eta_2$  meeting  $\alpha_2$  perpendicularly on both sides of  $\alpha_2$ . This arc can be seen in *Figure 7*. Now  $\alpha_2$  and  $\alpha_1$  intersect exactly once under the

angle  $\theta$ . Consider a right-angled triangle with sides of length  $\frac{\ell(\alpha_1)}{2}, r_2$  and  $\frac{\ell(\eta_2)}{2}$ . Here  $r_2$  contains information about the twist parameter  $tw_2$  with respect to  $\alpha_2$ . We get:

$$\cos(\theta) = \tanh(r_2) \coth\left(\frac{\ell(\alpha_1)}{2}\right).$$

Together with Equation (19), we obtain:

$$\tanh(r_2) = \frac{\tanh\left(\frac{\ell(\alpha_1) \cdot |tw_1|}{2}\right) \coth\left(\frac{\ell(\alpha_2)}{2}\right)}{\coth\left(\frac{\ell(\alpha_1)}{2}\right)} \quad \text{and} \quad |tw_2| = \min\left(\frac{2r_2}{\ell(\alpha_2)}, 1 - \frac{2r_2}{\ell(\alpha_2)}\right).$$

We will now look for a suitable  $\alpha_{12}$ . Consider again the lifts of  $\alpha_1$  in *Figure 7*. Consider the two points,  $q' \in \alpha_1'$  and  $q^* \in \alpha_1^*$  on the opposite side of  $s'$  and  $s^*$  with respect to the intersection point with  $\eta_1$  and at distance  $\ell(\alpha_1) - r_1$  from  $\eta_1'$ .  $q'$  and  $q^*$  are mapped to the same point  $q \in \mathcal{Q}_1$  by the covering map. Connecting these points we obtain a geodesic arc  $\alpha_{12}'$ , which maps to a simple closed geodesic  $\alpha_{12}$  in  $\mathcal{Q}_1$ . It follows from its intersection properties with  $\alpha_1$  and  $\alpha_2$  that  $\alpha_{12}$  is in the free homotopy class  $\alpha_1(\alpha_2)^{-1}$ . Using the same reasoning as for  $\alpha_2$ , we can find its length and the twist parameter  $tw_{12}$ , which leads to **Lemma 4.2**.  $\square$

## 4.2 Upper bounds for the energy of dual harmonic forms based on Q-pieces

We will establish estimates for all entries of the period Gram matrix based on the geometry of the Q-pieces  $(\mathcal{Q}_i)_{i=1,3,\dots,2g-1}$ . Following the approach given in Section 3, it is sufficient to construct suitable functions on

$$S_\gamma \cap \mathcal{Q}_i, \quad \text{where } \gamma \in \{\alpha_i, \alpha_{\tau(i)}, \alpha_{i\tau(i)}\}, \quad \text{for } i \in \{1, 3, \dots, 2g-1\}.$$

In this and the following subsection, we will only show how to obtain estimates for  $E(\sigma_1) = p_{11}$  based on the geometry of  $\mathcal{Q}_1$ . These estimates will only depend on the Fenchel-Nielsen coordinates  $(\ell(\beta_1), \ell(\alpha_2), tw_2)$  of  $\mathcal{Q}_1$ . In the same way, we obtain estimates for  $E(\sigma_2) = p_{22}$  based on the coordinates  $(\ell(\beta_1), \ell(\alpha_1), tw_1)$ , and for  $E(\sigma_1 + \sigma_2)$  based on the coordinates  $(\ell(\beta_1), \ell(\alpha_{12}), tw_{12})$ . Proceeding the same way on the remaining Q-pieces and combining these estimates as described in Section 3.2 (see Equations (12),(15) and (16)) we finally obtain estimates for all entries of the period matrix.

To obtain an upper bound for  $p_{11}$ , we embed  $S_{\alpha_2} \cap \mathcal{Q}_1$  into a hyperbolic cylinder  $C$  with baseline  $\alpha_2$  and denote this embedding by the same name. To obtain an estimate on  $E(\sigma_1)$ , we will give a parametrization of

$$S_{\alpha_2} \cap \mathcal{Q}_1 \subset C$$

based on a decomposition into trirectangles. To obtain this parametrization, we first cut open  $\mathcal{Q}_1$  along  $\alpha_2$  to obtain the Y-piece  $\mathcal{Y}_1$  with boundary geodesics  $\beta = \beta_1, \alpha_2^1$  and  $\alpha_2^2$ . Both  $\alpha_2^1$  and  $\alpha_2^2$  have length  $\ell(\alpha_2)$  (see *Figure 8*).

Denote by  $b$  the shortest geodesic arc connecting  $\alpha_2^1$  and  $\alpha_2^2$ . We cut open  $\mathcal{Y}_1$  along the shortest geodesic arcs connecting  $\beta$  and the other two boundary geodesics. We call  $\mathcal{O}_1$  the octagon, which we obtain by cutting open  $\mathcal{Y}_1$  along these lines. By abuse of notation, we denote the geodesic arcs in  $\mathcal{O}_1$  by the same letter as in  $\mathcal{Y}_1$ . The geodesic arc  $b$  divides  $\mathcal{O}_1$  into two isometric hexagons  $\mathcal{H}_1$  and  $\mathcal{H}_2$ . This decomposition is also shown in *Figure 8*.

In  $\mathcal{H}_1$   $b$  is the boundary geodesic connecting  $\frac{\alpha_2^1}{2}$  and  $\frac{\alpha_2^2}{2}$ . Denote by  $\delta^1$  the shortest geodesic arc in  $\mathcal{H}_1$  connecting  $b$  and the side opposite of  $b$  of length  $\frac{\ell(\beta)}{2}$ . By abuse of notation, we denote

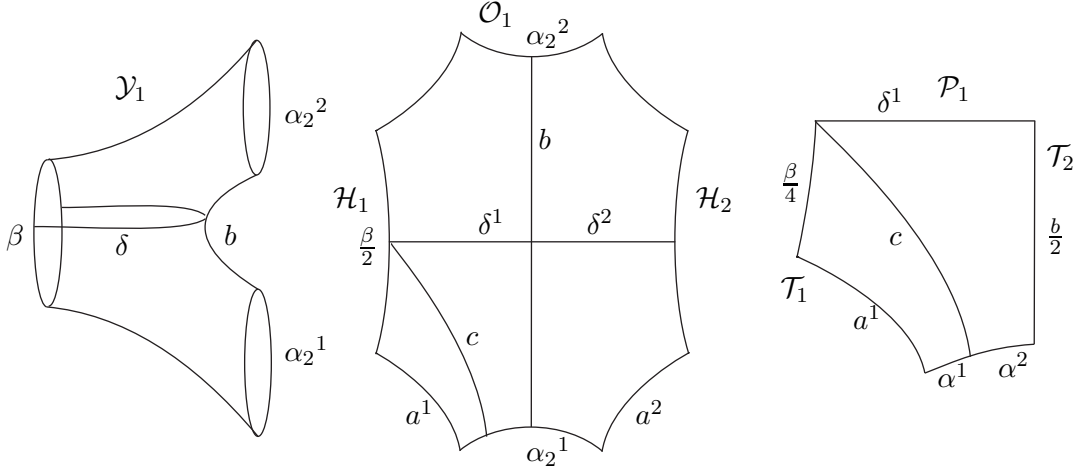


Figure 8: Decomposition of  $\mathcal{Y}_1$  into isometric hexagons  $\mathcal{H}_1$  and  $\mathcal{H}_2$

this side by  $\frac{\beta}{2}$ . We denote by  $\delta^2$  the arc in  $\mathcal{H}_2$  corresponding to  $\delta^1$  in  $\mathcal{H}_1$ . Let  $\delta = \delta^1 \cup \delta^2$  be the geodesic arc in  $\mathcal{O}_1$  formed by  $\delta^1$  and  $\delta^2$ . By abuse of notation, we denote the corresponding arc in  $\mathcal{Q}_1$  and  $\mathcal{Y}_1$  that maps to  $\delta^1 \cup \delta^2$  in  $\mathcal{O}_1$  also by  $\delta$ . It follows from the symmetry of  $\mathcal{Y}_1$  that  $\delta$  constitutes the intersection of the cut locus of  $\alpha_2$  with  $\mathcal{Q}_1$ :

$$\delta = CL(\alpha_2) \cap \mathcal{Q}_1.$$

Let  $a^1$  denote the geodesic arc connecting  $\frac{\alpha_2^1}{2}$  and  $\frac{\beta}{2}$  in  $\mathcal{H}_1$ , and  $a^2$  the corresponding arc in  $\mathcal{H}_2$  of the same length  $\ell(a^1) = \ell(a^2) = a$ .  $\delta^1$  divides  $\mathcal{H}_1$  into two isometric right-angled pentagons  $\mathcal{P}_1$  and  $\mathcal{P}_2$ . Let  $\mathcal{P}_1$  be the pentagon that has  $\frac{\alpha_2^1}{2}$  as a boundary. To establish the parametrization for  $S_{\alpha_2} \cap \mathcal{Q}_1$ , we divide  $\mathcal{P}_1$  into two trirectangles. Let  $c$  be the geodesic arc in  $\mathcal{P}_1$  that emanates from the vertex, where  $\frac{\beta}{2}$  and  $\delta^1$  intersect and that meets  $\frac{\alpha_2^1}{2}$  perpendicularly. It divides  $\frac{\alpha_2^1}{2}$  into two parts,  $\alpha^1$  and  $\alpha^2$  (see *Figure 8*).  $c$  divides  $\mathcal{P}_1$  into two trirectangles  $\mathcal{T}_1$  and  $\mathcal{T}_2$ , that have boundaries  $\alpha^1$  and  $\alpha^2$ , respectively.

To obtain an upper bound for  $p_{11}$ , we need to know the geometry of  $\mathcal{T}_1$  and  $\mathcal{T}_2$ . Hence, we need to know the lengths  $a$ ,  $\ell(\alpha^1)$ ,  $\ell(\alpha^2)$ , and  $\frac{\ell(b)}{2}$ . In the following subsection we will also need the length  $\ell(c)$  of  $c$ , which we will calculate here. To obtain these lengths, we will use the geometry of  $\mathcal{H}_1$ ,  $\mathcal{P}_1$ ,  $\mathcal{T}_1$  and  $\mathcal{T}_2$ . All formulas for the geometry of hyperbolic polygons are given in Section 2.2.

From the geometry of the hyperbolic pentagon  $\mathcal{P}_1$  we have:

$$\sinh\left(\frac{\ell(b)}{2}\right) = \frac{\cosh\left(\frac{\ell(\beta)}{4}\right)}{\sinh\left(\frac{\ell(\alpha_2)}{2}\right)} \quad (20)$$

$$\cosh(\ell(\delta^1)) = \sinh\left(\frac{\ell(\alpha_2)}{2}\right) \sinh(a). \quad (21)$$

Hence, we can express  $\ell(b)$  in terms of  $\ell(\alpha_2)$  and  $\ell(\beta)$ .

We obtain  $a$ , in terms of  $\ell(b)$  and  $\ell(\alpha_2)$ , from the geometry of the hyperbolic hexagon  $\mathcal{H}_1$  and



obtain a concrete lower bound  $f^l(FN_2)$  for

$$p_{11} = E_S(F_1) > E_B(F_1) \geq f^l(FN_2), \quad \text{where } B = B_2 = S_2^{\text{red}} \cap \mathcal{C}_2.$$

We will give a suitable construction for  $B = S_2^{\text{red}} \cap \mathcal{C}_2$  in Section 4.3.1. To this end, we lift  $\mathcal{C}_2$  into the universal covering as in the previous subsection (see *Figure 9*). We use the same notation for the geodesic arcs that occur. The important cut-out from *Figure 9* is depicted in *Figure 10*.

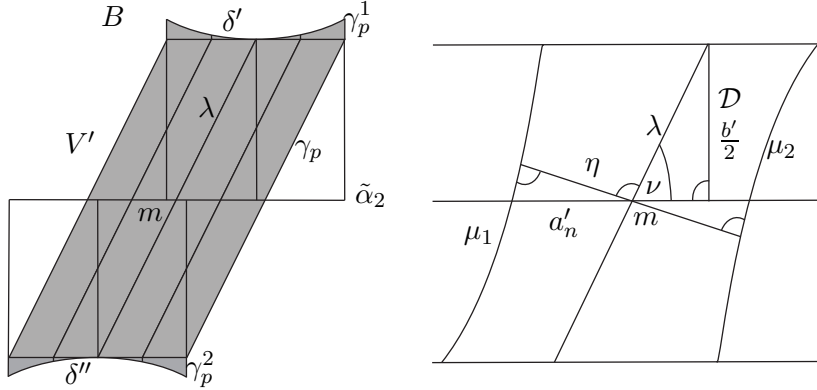


Figure 10: The area  $B$  (grey) and the construction of skewed Fermi coordinates  $\psi^\nu$

Let  $B$  be the grey hatched subset in the lift of  $\mathcal{C}_2$  in *Figure 10*. We will now give an exact description and parametrization of  $B$ .

#### 4.3.1 Parametrization of $B = S_2^{\text{red}} \cap \mathcal{C}_2$

The boundary of  $B$  contains the lines  $\delta'$  and  $\delta''$ . For each point  $p_1 \in \delta'$ , there exists a point  $p_2 \in \delta''$ , such that  $p_1$  and  $p_2$  map to the same point  $p$  on  $\delta \subset \mathcal{Q}_1$ . We may assume, without loss of generality, that

$$F_1(p_2) - F_1(p_1) = 1 \quad \text{for all } p_1 \in \delta'.$$

We will describe  $B$  as a union of lines, where each line  $l_p$  connects  $p_1$  and  $p_2$ . The line  $l_p$  is defined as follows. From  $p_1$  we go along the geodesic that meets  $\tilde{\alpha}_2$  perpendicularly until we meet  $\partial Z_{\frac{\ell(b)}{2}}(\tilde{\alpha}_2)$ , the boundary of the collar  $Z_{\frac{\ell(b)}{2}}(\tilde{\alpha}_2)$  (see definition (5)). We call this intersection point  $p'_1$  and the geodesic arc that forms  $\gamma_p^1$ . Let  $p'_2$  be the point on  $\partial Z_{\frac{\ell(b)}{2}}(\tilde{\alpha}_2)$  on the other side of  $\tilde{\alpha}_2$  that can be reached analogously, starting from  $p_2$ . We now go along the geodesic arc that connects  $p'_1$  and  $p'_2$ . We call this arc  $\gamma_p$ . Then from  $p'_2$ , we move along the geodesic arc connecting  $p'_2$  and  $p_2$ . We call this arc  $\gamma_p^2$ . We define  $l_p$  as the line traversed in this way. Let  $B$  be the disjoint union of these lines:

$$B = \bigsqcup_{p \in \delta} \{l_p\}$$

Let  $\lambda$  be the geodesic arc connecting the midpoints of  $\delta'$  and  $\delta''$ , and let  $m$  be the midpoint of  $\lambda$ . We will use a bijective parametrization  $\varphi$  of  $B$ :

$$\varphi : (t, s) \mapsto \varphi(t, s), \quad \text{such that}$$

- $\varphi(0, 0) = m$
- for all  $t \in [-\ell(\alpha^2), \ell(\alpha^2)]$ ,  $\varphi(t, 0) \in \tilde{\alpha}_2$  has directed distance  $t$  from  $m$
- for a fixed  $t_0 \in [-\ell(\alpha^2), \ell(\alpha^2)]$ ,  $\varphi(t_0, \cdot)$  parametrizes the line  $l_p$  that traverses  $\tilde{\alpha}_2$  in a point with directed distance  $t_0$  from  $m$  by arc length.

We parametrize the sets  $\bigcup_{p \in \delta} \{\gamma_p^1\}$  and  $\bigcup_{p \in \delta} \{\gamma_p^2\}$  in Fermi coordinates with baseline  $\tilde{\alpha}_2$ . The proper parametrization can be deduced from the geometry of the trirectangle  $\mathcal{T}_2$ .

We will parametrize  $Z_{\frac{\ell(b)}{2}}(\tilde{\alpha}_2) \cap B = \bigcup_{p \in \delta} \{\gamma_p\}$  using *skewed Fermi coordinates*  $\psi^\nu$ , with angle  $\nu$  and baseline  $\tilde{\alpha}_2$ . These are defined in the same way as the usual Fermi coordinates  $\psi$  (see Section 2.1), but instead of moving along geodesics emanating perpendicularly from the baseline, we move along geodesics that meet the baseline under the angle  $\nu$ . We will not give these coordinates explicitly, but will derive the essential information from the usual Fermi coordinates  $\psi$ .

We remind the reader that  $\lambda$  is the geodesic arc connecting the midpoints of  $\delta'$  and  $\delta''$ . Its midpoint  $m$  and the endpoints of  $\frac{b'}{2}$  are the vertices of a right-angled triangle  $\mathcal{D}$  (see *Figure 10*). In our case the angle  $\nu$  for the coordinates  $\psi^\nu$  is the angle of  $\mathcal{D}$  at the midpoint  $m$ . It follows from the geometry of right-angled triangles that

$$\cosh\left(\frac{\ell(\lambda)}{2}\right) = \cosh\left(\frac{\ell(b)}{2}\right) \cosh\left(\frac{\ell(\alpha_2)|tw_2|}{2}\right), \quad (22)$$

where we assume, without loss of generality, that the twist parameter  $tw_2$  is in the interval  $[0, \frac{1}{2}]$ . Otherwise the situation is symmetric to the depicted one. Using the geometry of the right-angled triangle  $\mathcal{D}$  we have:

$$\sin(\nu) = \frac{\sinh\left(\frac{\ell(b)}{2}\right)}{\sqrt{\cosh\left(\frac{\ell(b)}{2}\right)^2 \cosh\left(\frac{\ell(\alpha_2)|tw_2|}{2}\right)^2 - 1}}. \quad (23)$$

Consider the following geodesic arcs in  $Z_{\frac{\ell(b)}{2}}(\tilde{\alpha}_2) \cap B$ . For a  $n \in \mathbb{N}$ , let  $a'_n$  be a geodesic arc of length  $\frac{2\alpha^2}{n}$  on  $\tilde{\alpha}_2$  with midpoint  $m$ .  $\lambda$  intersects  $a'_n$  in  $m$  under the angle  $\nu$ . This is depicted in *Figure 10*.

Let  $\eta'$  be a geodesic intersecting  $\lambda$  perpendicularly in  $m$ . Let  $\mu_1$  and  $\mu_2$  be two geodesic arcs with endpoints on  $Z_{\frac{\ell(b)}{2}}(\tilde{\alpha}_2)$  that intersect  $\eta'$  perpendicularly, such that each of the arcs passes through an endpoint of  $a'_n$  on each side of  $\lambda$ . Let  $\eta$  be the geodesic arc on  $\eta'$  with endpoints on  $\mu_1$  and  $\mu_2$ . For fixed  $n \in \mathbb{N}$ , we denote by  $\eta_n$  the length of  $\eta$  and by  $\mu^n$  the length of  $\mu_1$  and  $\mu_2$ :

$$\eta_n = \ell(\eta) \quad \text{and} \quad \mu^n = \ell(\mu_1) = \ell(\mu_2).$$

By choosing usual Fermi coordinates with baseline  $\eta$ , we can parametrize the strip, whose boundary lines are  $\mu_1$  and  $\mu_2$  and two segments of  $\partial Z_{\frac{\ell(b)}{2}}(\tilde{\alpha}_2)$  (see *Figure 10*).

$n$  such strips can be aligned next to each other to obtain a parametrization of  $Z_{\frac{\ell(b)}{2}}(\tilde{\alpha}_2) \cap B$ . For  $n \rightarrow \infty$  we obtain a parametrization  $\psi^\nu$  of  $Z_{\frac{\ell(b)}{2}}(\tilde{\alpha}_2) \cap B$ . We get:

$$\lim_{n \rightarrow \infty} n \cdot \eta_n = \sin(\nu) 2\ell(\alpha^2) \quad \text{and} \quad \lim_{n \rightarrow \infty} \mu^n = \ell(\lambda).$$

Combining the parametrizations for the several pieces of  $B$ , we may assume that we have a parametrization  $\varphi$  that satisfies our conditions. For practical purposes, we extend the parametrization  $\varphi$  to the geodesics meeting  $\partial Z_{\frac{\ell(b)}{2}} \cap B$  perpendicularly in the direction opposite of  $\tilde{\alpha}_2$ .

### 4.3.2 Evaluating the lower bound for $p_{11} = E_S(F_1)$

Consider a point  $p_1 = \varphi(t_0, -x) \in \delta'$  and  $p_2 = \varphi(t_0, x) \in \delta''$ . The function  $F_1$  satisfies the boundary conditions  $F_1(p_1) = 1 + \tilde{c}$  and  $F_1(p_2) = \tilde{c}$ , where  $\tilde{c}$  is a constant. As we will see in the following, the constant  $\tilde{c}$  is not important for our estimate and we assume that  $\tilde{c} = 0$ .

We consider the strip  $V$ , where

$$V = \varphi([t_0 - \epsilon, t_0] \times [-x, x]), \quad \text{where } \epsilon > 0 \text{ if } t_0 < 0 \text{ and } \epsilon < 0 \text{ if } t_0 > 0.$$

We will show how to obtain a lower bound for the energy of  $F_1|_V$ ,  $E_V(F_1)$  for a sufficiently small  $\epsilon$ . We can align these strips to obtain a lower bound for  $E_B(F_1) \leq E(F_1)$ . We derive a lower bound for the energy of  $F_1|_V$ , assuming that

$$\begin{aligned} F_1|_{\varphi([t_0 - \epsilon, t_0] \times \{-x\})} &= F_1(p_1) = 0 \quad \text{and} \quad F_1|_{\varphi([t_0 - \epsilon, t_0] \times \{x\})} = F_1(p_2) = 1 \quad \text{and} \\ F_1|_{\varphi([t_0 - \epsilon, t_0] \times \{-\frac{\ell(\lambda)}{2}\})} &= F_1(p'_1) = a'_1 \quad \text{and} \quad F_1|_{\varphi([t_0 - \epsilon, t_0] \times \{\frac{\ell(\lambda)}{2}\})} = F_1(p'_2) = a'_2. \end{aligned}$$

Consider the subset  $V'$  of  $V$  given by

$$V' = \varphi([t_0 - \epsilon, t_0] \times [\frac{-\ell(\lambda)}{2}, \frac{\ell(\lambda)}{2}]).$$

Let  $F_{t_0} = f_{t_0} \circ \psi^\nu$  be a function defined on  $V'$  that realizes the minimum

$$\min_{V'} \left\{ \int_{V'} \|p_\varphi(Df)\|_2^2 \mid f \in \text{Lip}(V'), f|_{\varphi([t_0 - \epsilon, t_0] \times \{-\frac{\ell(\lambda)}{2}\})} = a_1 \text{ and } f|_{\varphi([t_0 - \epsilon, t_0] \times \{\frac{\ell(\lambda)}{2}\})} = a_2 \right\} \quad (\text{see (9)}).$$

Considering skewed Fermi coordinates as a limit case of Fermi coordinates with respect to an imaginary baseline  $\eta$ , and by applying the calculus of variations (see [Ge], p. 14-16) to the last integral in Equation (2), we obtain  $f_{t_0}$  as follows:

$$f_{t_0}(t, s) = \frac{a_2 - a_1}{H(\frac{\ell(\lambda)}{2}) - H(-\frac{\ell(\lambda)}{2})} H(s) + \frac{a_1 H(\frac{\ell(\lambda)}{2}) - a_2 H(-\frac{\ell(\lambda)}{2})}{H(\frac{\ell(\lambda)}{2}) - H(-\frac{\ell(\lambda)}{2})},$$

where  $H(s) = 2 \operatorname{arctanh}(\exp(s))$ . The energy  $E_{V'}(p_\varphi(DF_{t_0}))$  is

$$E_{V'}(p_\varphi(DF_{t_0})) = \frac{(a_2 - a_1)^2 \sin(\nu) |\epsilon|}{2(\operatorname{arctan}(\exp(\frac{\ell(\lambda)}{2})) - \operatorname{arctan}(\exp(-\frac{\ell(\lambda)}{2})))} = k_1 (a_2 - a_1)^2 |\epsilon|. \quad (24)$$

We can extend  $F_{t_0}$  to a function on  $V$  that satisfies the boundary conditions

$$F_{t_0}|_{\varphi([t_0 - \epsilon, t_0] \times \{\pm x\})} = F_1|_{\varphi([t_0 - \epsilon, t_0] \times \{\pm x\})}.$$

As before, we choose  $F_{t_0}$  such that it minimizes  $E_{V \setminus V'}(p_\varphi(D(\cdot)))$  with the given boundary conditions. We have with  $E_{V \setminus V'}(p_\varphi(DF_{t_0})) = E_{V \setminus V'}(F_{t_0})$ :

$$E_{V \setminus V'}(F_{t_0}) = \frac{(a_1^2 + (1 - a_2)^2)|\epsilon|}{2(\arctan(\exp(x(t_0))) - \arctan(\exp(\frac{\ell(b)}{2})))} = k_2(t_0)(a_1^2 + (1 - a_2)^2)|\epsilon|, \quad (25)$$

where  $x(t_0) = \ell(\gamma_p^1) + \frac{\ell(b)}{2}$ , such that  $\varphi(t_0, \cdot)$  parametrizes the line  $l_p$ . For  $a_1 = a'_1 = F_1(p'_1)$  and  $a_2 = a'_2 = F_1(p'_2)$ , we have by construction  $E_V(F_1) \geq E_V(p_\varphi(DF_{t_0}))$ .

Though we do not know the values  $a'_1$  and  $a'_2$ , we obtain a lower bound of the energy of  $F_1$  on  $V$ , if we determine the values  $F_{t_0}(p'_1) = c_1 = c_1(t_0)$  and  $F_{t_0}(p'_2) = c_2 = c_2(t_0)$ , respectively, such that these values are minimizing the total energy  $E_V(p_\varphi(F_{t_0}))$ . As the two arcs  $\gamma_p^1$  and  $\gamma_p^2$  have the same length, we have to solve the following problem:

Find  $c_1, c_2$ , such that  $1 - c_2 = c_1 \Leftrightarrow (c_2 - c_1) = 1 - 2c_1$ , and

$$E_V(p_\varphi(DF_{t_0})) = E_{V'}(p_\varphi(DF_{t_0})) + E_{V \setminus V'}(F_{t_0})$$

is minimal. We obtain from Equations (24) and (25) that  $c_1 = \frac{k_1}{k_2(t_0) + 2k_1}$ . We can cover  $B$  with a set of such strips  $V_{t_0} = V$ , such that these intersect only on the boundary and combine the  $F_{t_0}|_{V_{t_0}}$  to a function  $f_1$  on  $B$ . We have  $E_V(F_1) \geq E_V(p_\varphi(Df_1))$ .

As we consider only the energy  $E_B(p_\varphi(Df_1))$  of the projection, the approximation is true in the limit case, where  $\epsilon \rightarrow 0$ . Due to the symmetry of the area  $B$  we obtain in total with  $c_1$  in Equations (24) and (25):

$$p_{11} = E(F_1) \geq E_B(p_\varphi(Df_1)) = 2 \int_{t=0}^{\ell(\alpha^2)} \frac{k_1 k_2(t)}{k_2(t) + 2k_1} dt = f^l(\ell(\beta_1), \ell(\alpha_2), tw_2). \quad (26)$$

$E_{V \setminus V'}(p_\varphi(DF_{t_0}))$  is monotonously decreasing if  $x(t_0) - \frac{\ell(b)}{2}$  in Equation (25) is increasing. Hence we find a simpler approximation for  $E(F_1)$ , setting  $x(t_0) := \ell(c') = \ell(c)$  (see *Figure 9*). In this case, we can set  $k_2(t) = k_2(\ell(\alpha^2))$  for all  $t$ . We obtain furthermore a simplified upper bound, if we define our test function only on  $Z_{w'}(\alpha_2)$ , where  $w' = \min\{a, \frac{\ell(b)}{2}\}$ . This upper bound  $f_{simp}^u$  corresponds to the method from [BS] applied to a Q-piece. The explicit formulas for  $f_{simp}^l$  and  $f_{simp}^u$  are summarized in inequality (30).

To obtain the lower bound  $f^l$  that depends only on  $\ell(\alpha_2), |tw_2|$ , and  $\ell(\beta_1)$  we first have to express  $\frac{\ell(b)}{2}$  and  $\ell(\lambda)$  and  $\nu$  in terms of these variables (see Equations (20),(22) and (23)). Using the parametrization of  $\mathcal{T}_2$  in Equation (25), we can then express  $f^l$  in terms of  $\ell(\alpha_2), |tw_2|$  and  $\ell(\beta_1)$ . This way we obtain explicit values in Equation (26). These formulas are summarized in the following subsection.

#### 4.4 Summary

In this section, we summarize the formulas from the previous subsections and outline our estimates in *Table 1* and *2*. We also give an example for our estimates in **Example 4.3**. First, we give a description of  $f^u$  and  $f^l$  from **Theorem 4.1**.

#### 4.4.1 Upper bound $f^u$ from Theorem 4.1

In the remaining part of this paper we fix the notation in the following way.

For  $j \in \{i, \tau(i), i\tau(i)\}$ , let  $\mathcal{Q}_i$  be a Q-piece given in Fenchel-Nielsen coordinates  $FN_j = (\ell(\beta_j), \ell(\alpha_j), tw_j)$ , where  $\beta_j = \beta_i$  is the boundary geodesic of  $\mathcal{Q}_i$ , and  $tw_j \in (-\frac{1}{2}, \frac{1}{2}]$  be the twist parameter at an interior simple closed geodesic  $\alpha_j$ . We have from Section 4.2:

$$\sinh\left(\frac{\ell(b)}{2}\right) = \frac{\cosh\left(\frac{\ell(\beta_j)}{4}\right)}{\sinh\left(\frac{\ell(\alpha_j)}{2}\right)} \quad (27)$$

$$\coth(a) = \tanh\left(\frac{\ell(b)}{2}\right) \cosh\left(\frac{\ell(\alpha_j)}{2}\right) \text{ and } \sinh(\ell(c)) = \frac{\cosh\left(\frac{\ell(\beta)}{4}\right)}{\sqrt{\tanh\left(\frac{\ell(b)}{2}\right)^2 \cosh\left(\frac{\ell(\alpha_j)}{2}\right)^2 - 1}} \quad (28)$$

$$\coth(\ell(\alpha^2)) = \cosh\left(\frac{\ell(b)}{2}\right)^2 \tanh\left(\frac{\ell(\alpha_j)}{2}\right) \text{ and } \ell(\alpha^1) = \frac{\ell(\alpha_j)}{2} - \ell(\alpha^2). \quad (29)$$

Using the above, we obtain a description of the cut locus  $CL(\alpha_j) \cap \mathcal{Q}_i$  in a cylinder  $\mathcal{C}_j$  in Fermi coordinates. Set  $\mathbb{S}_{\alpha_j}^1 = \mathbb{R} \text{ mod } (t \mapsto t + \ell(\alpha_j))$ . For  $l \in \{1, 2\}$  let

$$a_l : \mathbb{S}_{\alpha_j}^1 \rightarrow \mathbb{R}, a_l : t \mapsto a_l(t)$$

be a parametrization of the two connected components of  $CL(\alpha_j) \cap \mathcal{Q}_i$  in  $\mathcal{C}_j$ . Then

$$\begin{aligned} a_2(t) : &= \begin{cases} \operatorname{arctanh}(\cosh(t - \ell(\alpha^2)) \tanh(\frac{\ell(b)}{2})) & \text{if } t \in (0, 2\ell(\alpha^2)] \\ \operatorname{arctanh}(\cosh(t - (2\ell(\alpha^2) + \ell(\alpha^1))) \tanh(\frac{\ell(b)}{2})) & \text{if } t \in (2\ell(\alpha^2), \ell(\alpha_j)] \end{cases} \\ a_1(t) : &= -a_2(t + |tw_j|) \end{aligned}$$

Applying **Theorem 2.1** to estimate the capacity of  $S_{\alpha_j} \cap \mathcal{Q}_i$  with boundary  $CL(\alpha_j) \cap \mathcal{Q}_i$ , we obtain:

$$\begin{aligned} f^u(N_j) &:= \int_{t=0}^{\ell(\alpha_j)} \frac{1 + \frac{1}{3} \cdot \left( \frac{(a_1'(t))^2}{\cosh^2(a_1(t))} + \frac{a_1'(t)}{\cosh(a_1(t))} \cdot \frac{a_2'(t)}{\cosh(a_2(t))} + \frac{(a_2'(t))^2}{\cosh^2(a_2(t))} \right)}{2(\arctan(\exp(a_2(t))) - \arctan(\exp(a_1(t))))} dt \geq \\ &\quad \operatorname{cap}(S_{\alpha_j} \cap \mathcal{Q}_i) \geq \\ &\quad \int_{t=0}^{\ell(\alpha_j)} \frac{1}{2(\arctan(\exp(a_2(t))) - \arctan(\exp(a_1(t))))} dt := f_{low}^u(FN_j), \end{aligned}$$

where  $f_{low}^u(FN_j)$  is a lower bound for the capacity of  $S_{\alpha_j} \cap \mathcal{Q}_i$ .

#### 4.4.2 Lower bound $f^l$ from Theorem 4.1

Based on Section 4.3, we first give a suitable construction for  $S_j^{red} \cap \mathcal{Q}_i$ , where  $j \in \{i, \tau(i), i\tau(i)\}$ . From Equations (22) and (23) we obtain (see *Figure 10*):

$$\cosh\left(\frac{\ell(\lambda)}{2}\right) = \cosh\left(\frac{\ell(b)}{2}\right) \cosh\left(\frac{\ell(\alpha_j)|tw_j|}{2}\right) \quad \text{and} \quad \sin(\nu) = \frac{\sinh\left(\frac{\ell(b)}{2}\right)}{\sqrt{\cosh\left(\frac{\ell(b)}{2}\right)^2 \cosh\left(\frac{\ell(\alpha_j)|tw_j|}{2}\right)^2 - 1}}.$$

Using the above we obtain a description of the cut locus  $CL(\alpha_j)^{red} \cap \mathcal{Q}_i$  in a cylinder  $\mathcal{C}_j$  in Fermi coordinates. Let

$$a_{red} : [0, 2\ell(\alpha^2)] \rightarrow \mathbb{R}, \quad a_{red} : t \mapsto a_{red}(t)$$

be a parametrization of one of the two connected components of  $CL(\alpha_j)^{red} \cap \mathcal{Q}_i$ . Then

$$a_{red}(t) := \operatorname{arctanh}\left(\cosh(t - \ell(\alpha^2)) \tanh\left(\frac{\ell(b)}{2}\right)\right) \quad \text{for } t \in [0, 2\ell(\alpha^2)]$$

From Equation (24) and (25) (see Section 4.3.2) we have:

$$\begin{aligned} k_1 &= \frac{\sin(\nu)}{2(\arctan(\exp(\frac{\ell(\lambda)}{2})) - \arctan(\exp(-\frac{\ell(\lambda)}{2})))} \\ k_2(t) : &= \frac{1}{2(\arctan(\exp(a_{red}(t))) - \arctan(\exp(\frac{\ell(b)}{2})))} \quad \text{for } t \in [0, 2\ell(\alpha^2)]. \end{aligned}$$

Finally, we obtain the lower bound  $f^l(FN_j)$  on  $E(\sigma_{\tau(j)})$ , where  $\sigma_{\tau(i\tau(i))} = \sigma_i + \sigma_{\tau(i)}$  from Equation (26):

$$E(\sigma_{\tau(j)}) \geq 2 \int_{t=0}^{\ell(\alpha^2)} \frac{k_1 k_2(t)}{k_2(t) + 2k_1} dt := f^l(FN_j).$$

We also provide here the simplified upper and lower bound  $f_{simp}^u(FN_j)$  and  $f_{simp}^l(FN_j)$ , respectively. For  $w' = \min\{a, \frac{\ell(b)}{2}\}$ :

$$f_{simp}^u(FN_j) = \frac{\ell(\alpha_j)}{2(\arctan(e^{w'}) - \arctan(e^{-w'}))} \geq E(\sigma_{\tau(j)}) \geq \frac{2\ell(\alpha^2)k_1 k_2(\ell(\alpha^2))}{k_2(\ell(\alpha^2)) + 2k_1} = f_{simp}^l(FN_j). \quad (30)$$

From  $(f^u(FN_j))_j$  and  $(f^l(FN_j))_j$  all entries of  $P_S$  can be calculated. This follows from Equations (12), (15), and (16).

The following two tables provide a comparison of the estimates for the energy of a harmonic form based on the geometry of a Q-piece  $\mathcal{Q}_i$ , given in Fenchel-Nielsen coordinates  $FN_j = (\ell(\beta_j), \ell(\alpha_j), tw_j)$ . Here  $tw_j = 0$  in Table 1 and  $tw_j = \frac{1}{4}$  in Table 2.

$\ell(\beta_j)$	$\ell(\alpha_j)$	$f_{simp}^u(FN_j)$	$f^u(FN_j)$	$f_{low}^u(FN_j)$	$f^l(FN_j)$	$f_{simp}^l(FN_j)$
1	1	0.45	0.55	0.42	0.40	0.32
	2	1.39	1.41	1.14	1.11	0.69
	5	14.81	8.70	8.17	8.13	1.83
	10	359.74	112.46	111.85	111.80	3.71
	20	106778.29	16772.11	16771.50	16771.45	7.39
2	1	0.44	0.47	0.41	0.33	0.29
	2	1.31	1.23	1.08	0.95	0.67
	5	13.57	7.87	7.49	7.30	2.00
	10	329.05	102.76	102.30	102.11	4.20
	20	97667.22	15340.96	15340.49	15340.22	8.53
5	1	0.43	0.44	0.40	0.12	0.11
	2	1.15	1.10	1.01	0.36	0.33
	5	8.26	5.41	5.17	3.82	1.81
	10	196.51	62.08	61.71	60.30	4.72
	20	58319.75	9161.19	9160.80	9159.37	10.46
10	1	0.46	0.58	0.42	0.01	0.01
	2	1.39	1.41	1.14	0.03	0.03
	5	10.82	6.41	6.13	0.65	0.57
	10	60.64	26.06	25.60	17.54	3.59
	20	17959.42	2828.11	2827.62	2819.53	9.90
20	1	0.46	0.69	0.42	0.000068	0.000068
	2	1.42	1.86	1.17	0.000212	0.000212
	5	15.21	9.18	8.41	0.004493	0.004493
	10	262.37	82.11	81.71	0.66	0.57
	20	1484.09	347.17	346.61	231.58	6.81

Table 1:  $tw_j = 0$ : Comparison of the estimates for the energy of a harmonic form based on the geometry of a Q-piece  $\mathcal{Q}_i$ , given in Fenchel-Nielsen coordinates  $FN_j = (\ell(\beta_j), \ell(\alpha_j), 0)$ , for  $j \in \{i, \tau(i), i\tau(i)\}$

$\ell(\beta_j)$	$\ell(\alpha_j)$	$f_{simp}^u(FN_j)$	$f^u(FN_j)$	$f_{low}^u(FN_j)$	$f^l(FN_j)$	$f_{simp}^l(FN_j)$
1	1	0.45	0.55	0.41	0.39	0.32
	2	1.39	1.43	1.12	1.00	0.65
	5	14.81	7.73	7.00	0.90	0.67
	10	359.74	61.96	60.94	0.04	0.04
	20	106778.29	2750.28	2749.10	0.00011	0.00011
2	1	0.44	0.47	0.40	0.33	0.29
	2	1.31	1.22	1.07	0.87	0.63
	5	13.57	6.92	6.44	0.91	0.70
	10	329.05	56.48	55.76	0.04	0.04
	20	97667.22	2515.41	2514.53	0.00012	0.00012
5	1	0.43	0.44	0.40	0.12	0.11
	2	1.15	1.10	1.01	0.34	0.32
	5	8.26	5.12	4.82	0.92	0.74
	10	196.51	35.62	35.11	0.06	0.06
	20	58319.75	1504.60	1503.90	0.00018	0.00018
10	1	0.46	0.59	0.42	0.010	0.010
	2	1.39	1.42	1.12	0.032	0.032
	5	10.82	5.78	5.46	0.41	0.37
	10	60.64	19.40	18.75	0.14	0.14
	20	17959.42	484.70	483.96	0.14	0.0005
20	1	0.46	0.72	0.42	0.000068	0.000068
	2	1.42	1.83	1.15	0.000205	0.000205
	5	15.21	8.32	7.21	0.003701	0.003701
	10	262.37	45.52	44.96	0.18	0.18
	20	1484.09	99.69	98.69	0.0042	0.0042

Table 2:  $tw_j = \frac{1}{4}$ : Comparison of the estimates for the energy of a harmonic form based on the geometry of a Q-piece  $\mathcal{Q}_i$ , given in Fenchel-Nielsen coordinates  $FN_j = (\ell(\beta_j), \ell(\alpha_j), \frac{1}{4})$ , for  $j \in \{i, \tau(i), i\tau(i)\}$

**Example 4.3** Let  $\mathcal{Q}_1$  and  $\mathcal{Q}_3$  be two isometric Q-pieces given in Fenchel-Nielsen coordinates  $FN_1$  and  $FN_3$ , respectively, where

$$FN_i = (\ell(\beta_i), \ell(\alpha_i), tw_i) = (2, 1, 0.1), \quad \text{for } i \in \{1, 3\},$$

where  $\beta_i$  is the boundary geodesic,  $\alpha_i$  an interior simple closed geodesic, and  $tw_i$  the twist parameter at  $\alpha_i$ . Let

$$S = \mathcal{Q}_1 + \mathcal{Q}_3$$

be a Riemann surface of genus 2, which we obtain by gluing  $\mathcal{Q}_1$  and  $\mathcal{Q}_3$  along  $\beta_1$  and  $\beta_3$  with arbitrary twist parameter  $tw_\beta \in (-\frac{1}{2}, \frac{1}{2}]$ . Then there exists a canonical basis  $A = (\alpha_1, \dots, \alpha_4)$  and a corresponding period Gram matrix  $P_S$ , such that

$$\begin{pmatrix} 2.11 & -0.46 & -0.42 & -0.26 \\ -0.46 & 0.33 & -0.26 & -0.11 \\ -0.42 & -0.26 & 2.11 & -0.46 \\ -0.26 & -0.11 & -0.46 & 0.33 \end{pmatrix} \leq P_S \leq \begin{pmatrix} 2.53 & 0.20 & 0.42 & 0.26 \\ 0.20 & 0.44 & 0.26 & 0.11 \\ 0.42 & 0.26 & 2.53 & 0.20 \\ 0.26 & 0.11 & 0.20 & 0.44 \end{pmatrix}.$$

This follows from **Theorem 4.1**. For the Q-piece  $\mathcal{Q}_1$  we obtain the following Fenchel Nielsen coordinates  $FN_j$  from **Lemma 4.2** and the corresponding estimates for  $f^u(FN_j)$  and  $f^l(FN_j)$ :

$j$	$\ell(\beta_j)$	$\ell(\alpha_j)$	$ tw_j $	$f_{simp}^u(FN_j)$	$f^u(FN_j)$	$f^l(FN_j)$
1	2	1	0.1	0.44	0.47	0.33
2	2	3.032	0.017	3.16	2.53	2.11
12	2	3.243	0.132	3.73	2.85	2.05

Table 3: A Q-piece  $\mathcal{Q}_1$  given in different Fenchel-Nielsen coordinates  $FN_j = (\ell(\beta_j), \ell(\alpha_j), tw_j)$  and the values of the corresponding functions  $f_{simp}^u(FN_j)$ ,  $f^u(FN_j)$  and  $f^l(FN_j)$

## Acknowledgement

The presented work was supported by the Alexander von Humboldt foundation. I would like to thank Peter Buser and Hugo Akrouit for helpful discussions and Paman Gujral for proofreading the manuscript.

## References

- [Ba] Bavard, C. : *Anneaux extrémaux dans les surfaces de Riemann*, *Manuscripta mathematica*, **117** (2005), 265–271.
- [BL] Birkenhake, Ch. and Lange, H. : *Complex Abelian varieties*, *Grundlehren der mathematischen Wissenschaften* (302), Springer-Verlag, Berlin Heidelberg New York, (2004).
- [BMMS] Buser, P., Makover, E., Muetzel, B. and Silhol, R. : *The Jacobian of Riemann surfaces with short simple closed geodesics* (2012) (in preparation)

- [BPS] Balacheff, F., Parlier H. and Sabourau, S. : *Short loop decompositions of surfaces and the geometry of Jacobians*, *Geom. Funct. Anal.* **22**(1) (2012), 37–73.
- [BS] Buser, P. and Sarnak, P. : *On the Period Matrix of a Riemann Surface of Large Genus (with an Appendix by Conway, J.H. And Sloane, N.J.A.)*, *Inventiones Mathematicae* **117**(1) (1994), 27–56.
- [BSe1] Buser, P. and Seppälä, M. : *Short homology bases and partitions of Riemann surfaces*, *Topology* **41**(5) (2002), 863–871.
- [BSe2] Buser, P. and Seppälä, M. : *Triangulations and homology of Riemann surfaces*, *Proc. Amer. Math. Soc.* **131**(2) (2003), 425–432.
- [BSi] Buser, P. and Silhol, R. : *Geodesics, Periods, and equations of real hyperelliptic curves*, *Duke M. J.* **108** (2001), 211–250.
- [Bu] Buser, P. : *Geometry and Spectra of compact Riemann surfaces*, *Progress in mathematics* (106), Birkhäuser Verlag, Boston, (1992).
- [FK] Farkas, H.M. and Kra, I. : *Riemann Surfaces 2nd edition*, Springer-Verlag, (1992).
- [Ge] Gelfand, I.M. : *Calculus of variations*, Dover Publications, New York, (2000).
- [GT] Goldshtein, V. and Troyanov, M. : *Capacities in metric spaces*, *Integral Equations and Operator Theory* **44** (2002), 212–242.
- [Mu1] Muetzel, B. : *Inequalities for the capacity of non-contractible annuli on cylinders of constant and variable negative curvature*, to appear in *Geometriae Dedicata*, DOI 10.1007/s10711-012-9788-z (2012)
- [Mu2] Muetzel, B. : *On the second successive minimum of the Jacobian of a Riemann surface*, *Geom. Dedicata* **161** (1) (2012), 85–107.
- [Pa] Parlier, H. : *On the geometry of simple closed geodesics*, PhD thesis, Ecole Polytechnique Fédérale de Lausanne, (2004).
- [Se] Seppälä, M. : *Computation of Period Matrices of Real Algebraic-Curves*, *Discrete and Computational Geometry* **11**(1) (1994), 65–81.